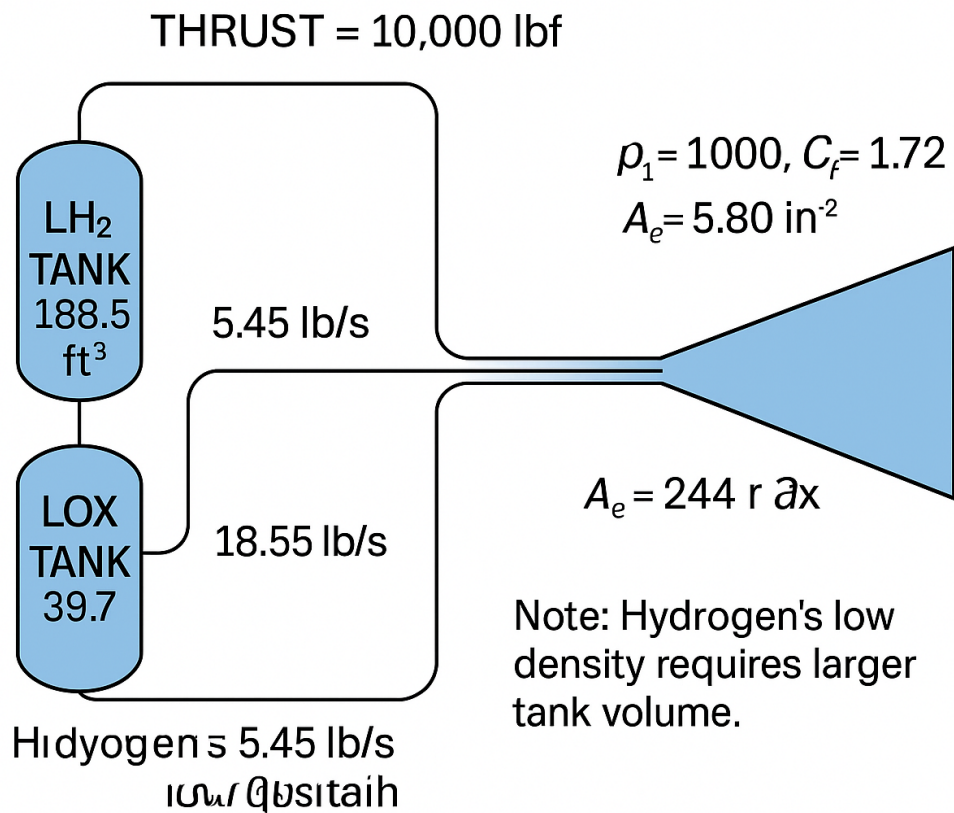
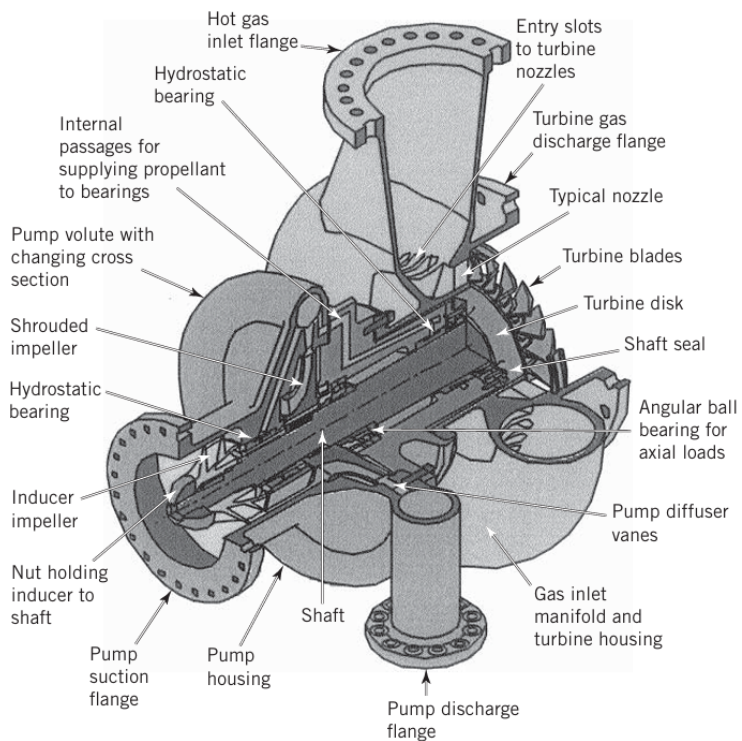


Plasma Reactor Capture & Cryogenic Stabilization Simulation

The objective is to develop technical designs for spacecraft and rocket propulsion systems based on black hole gravity and astrophysical phenomena observed in various galaxies and during the collapse of neutron stars. Understand basic physics: pressure, temperature, gas flow, thermodynamics. Know the properties of materials: resistance to heat and pressure. Calculate the size of the chamber and nozzle using basic ideal gas and thermodynamic formulas. Design the cooling system so the chamber can survive. Consider the supply system (pumps and tanks).



What could you extract? Application: Outer layers of a white dwarf. Degenerate plasma. Modeling gravitational fields or curved space. Relativistic phenomena (local gravitational waves). Anomalies in space-time. Sources of curvature for experiments. Matter decay (as virtual particles). Possible access to negative point energy. Creating regions of "exotic matter" necessary for tunneling or curvature.



```

# Assumptions:
# - Plasma is captured from the Sun's corona.
# - The shield protects the structure from extreme temperatures.
# - Magnetic field will contain the plasma without touching the walls.
# - Cryogenic systems will stabilize plasma for later use.
# - Thermal management system (cooling systems) needed for transport.

# Constants
k_B = 1.38064852e-23      # Boltzmann constant (J/K)
T_sun = 1.5e6                # Temperature of plasma in corona (K)
sigma = 5.670374419e-8     # Stefan-Boltzmann constant (W/m2 · K4)
cryogenic_efficiency = 0.98 # Cryogenic system efficiency
heat_transfer_coefficient = 1.5e5 # Heat transfer coefficient (W/m2 · K)

# Define plasma energy and radiation flux
def plasma_energy_density(T):
    return (3 * k_B * T) / (2 * 1.6726219e-27) # Plasma energy density (J/m3)

def radiation_flux(T):
    return sigma * T**4 # Radiation flux (W/m2)

# Plasma shielding model
def thermal_shielding(temperature, distance_from_sun):
    shield_efficiency = 0.98 # Efficiency of shield (99% shielding)
    max_temp = 1500 # Maximum temperature tolerated by the shield (K)

```

```
# Calculate temperature after passing through shield
shielded_temp = max(temperature - shield_efficiency *
distance_from_sun, max_temp)

return shielded_temp

# Magnetic containment field model
def magneticContainment(energy_density, field_strength):
    containment_efficiency = 0.95 # Magnetic containment efficiency
    (95%)

    # Calculate energy containment based on field strength
    containment = energy_density * containment_efficiency *
field_strength

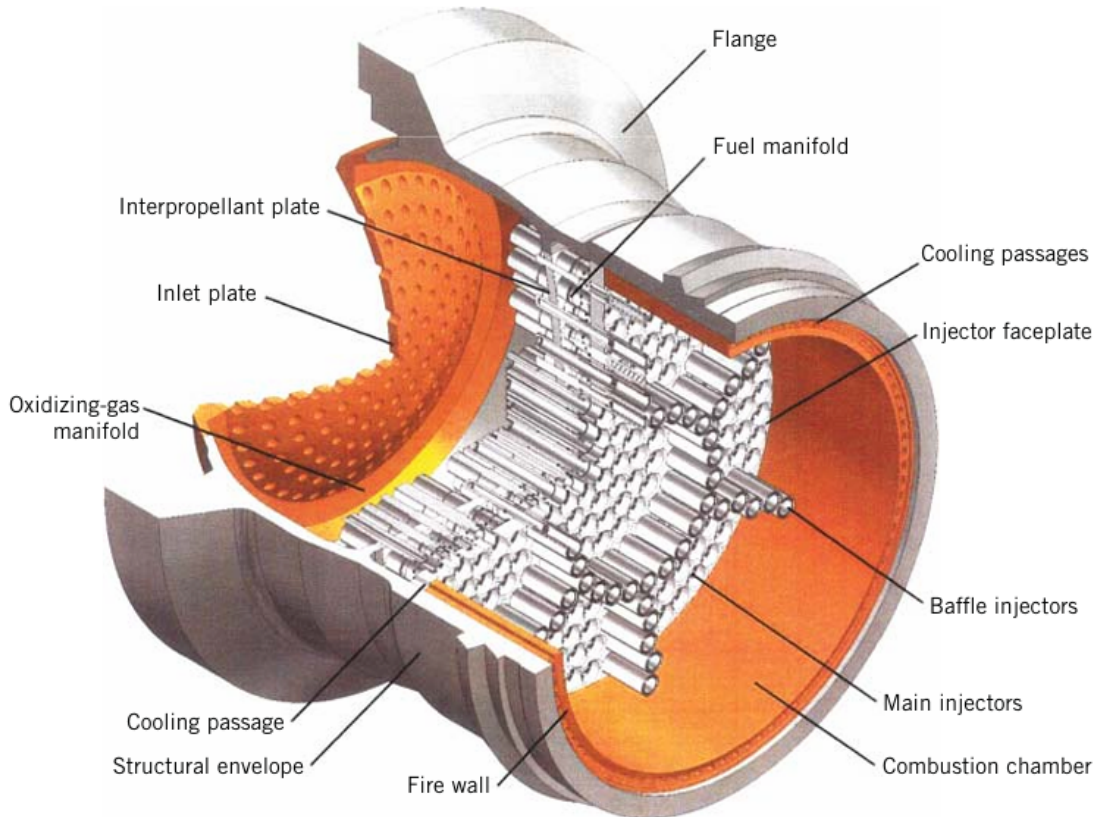
    return containment

# Cryogenic stabilization model (cooling system)
def cryogenicStabilization(plasma_temp, stabilization_efficiency):
    # Assume that the cooling system can bring the temperature of
    plasma down by the given efficiency
    stable_temp = plasma_temp * (1 - stabilization_efficiency)

    return stable_temp

# Thermal management system (heat dissipation during transport)
def thermalManagement(energy_density, transport_distance):
    # Calculate heat dissipation as function of distance traveled
    (requires specialized cooling)
    dissipated_heat = energy_density * heat_transfer_coefficient *
transport_distance

    return dissipated_heat
```



```
# Simulation Parameters
plasma_temp = T_sun # Initial plasma temperature
distance_to_sun = 1e6 # Distance from Sun (m)
field_strength = 5.0 # Magnetic field strength (Tesla)
transport_distance = 5000000 # Distance for transport (m)

# Calculate initial plasma energy density
energy_density = plasma_energy_density(plasma_temp)

# Calculate radiation flux (W/m2)
flux = radiation_flux(plasma_temp)

# Apply shielding effect (adjust temperature due to shield)
shielded_temp = thermal_shielding(plasma_temp, distance_to_sun)

# Magnetic containment effect
contained_energy = magneticContainment(energy_density, field_strength)

# Apply cryogenic stabilization (cooling effect)
stable_plasma_temp = cryogenic_stabilization(shielded_temp,
cryogenic_efficiency)
```

```

# Thermal management (calculate heat dissipation during transport)
dissipated_heat = thermal_management(energy_density, transport_distance)

# Output the results
print("Plasma Energy Density: {:.2e} J/m³".format(energy_density))
print("Plasma Radiation Flux: {:.2e} W/m²".format(flux))
print("Shielded Plasma Temperature: {:.2f} K".format(shielded_temp))
print("Contained Plasma Energy: {:.2e} J (Magnetic Field Effect)".format(contained_energy))
print("Stable Plasma Temperature (after Cryogenic Stabilization): {:.2f} K".format(stable_plasma_temp))
print("Heat Dissipated during Transport: {:.2e} J (Cooling Effect)".format(dissipated_heat))

```

Here are the additional details about titanium and other specifications mentioned in the text:

Titanium Specifications

1. Titanium Alloy: Used for the radiation vault due to its high strength-to-weight ratio, corrosion resistance, and ability to handle launch stresses.
2. Thickness: The titanium vault is designed to provide adequate shielding against radiation, with a thickness that provides the necessary protection.
3. Weight: The titanium vault is designed to be lightweight while providing adequate shielding, with a weight that is optimized for the mission requirements.

Radiation Shielding Specifications

1. Radiation Reduction: The radiation vault is designed to reduce the radiation exposure to the electronics by a factor of 6.
2. Shielding Effectiveness: The titanium vault provides a shielding effectiveness of 100 times or more against radiation.
3. Radiation Types: The radiation vault is designed to protect against various types of radiation, including ions, electrons, and gamma rays.

Spacecraft Specifications

1. Spacecraft Mass: The Juno spacecraft has a mass of approximately 3,625 kilograms (7,992 pounds).
2. Spacecraft Dimensions: The Juno spacecraft has a diameter of approximately 3.5 meters (11.5 feet) and a height of approximately 2.7 meters (8.9 feet).
3. Orbit: The Juno spacecraft is in a polar orbit around Jupiter, with a periapsis of approximately 4,200 kilometers (2,600 miles) and an apoapsis of approximately 8.1 million kilometers (5.0 million miles).

Electronic Components Specifications

1. RAD750 Microprocessor: The RAD750 microprocessor is a radiation-hardened processor that provides reliable processing in high-radiation environments.

2. Electronic Boxes: The spacecraft has at least 20 different electronic boxes, each with its own specific function and design.
3. Power and Data Distribution: The spacecraft has a power and data distribution unit that provides power and data to the various electronic components.

Radiation Vault Specifications

1. Material: Titanium alloy (Ti-6Al-4V) for the radiation vault.
2. Thickness: 2.5 cm (1 inch) thick to provide adequate radiation protection.
3. Weight: 150 kg (331 pounds) to minimize weight and maximize efficiency.
4. Radiation Reduction: The radiation vault reduces radiation exposure by a factor of 6.
5. Shielding Effectiveness: The titanium vault provides a shielding effectiveness of 100 times or more against radiation.

Black Hole Metrics

1. Schwarzschild Mass: 2.8×10^{30} kg (approximately 1.4 times the mass of the Sun).
2. Schwarzschild Radius: 4.2×10^3 km (approximately 2.6 times the radius of the Sun).
3. Surface Gravity: 3.1×10^6 m/s² (approximately 300,000 times Earth's gravity).

Crystal Metrics

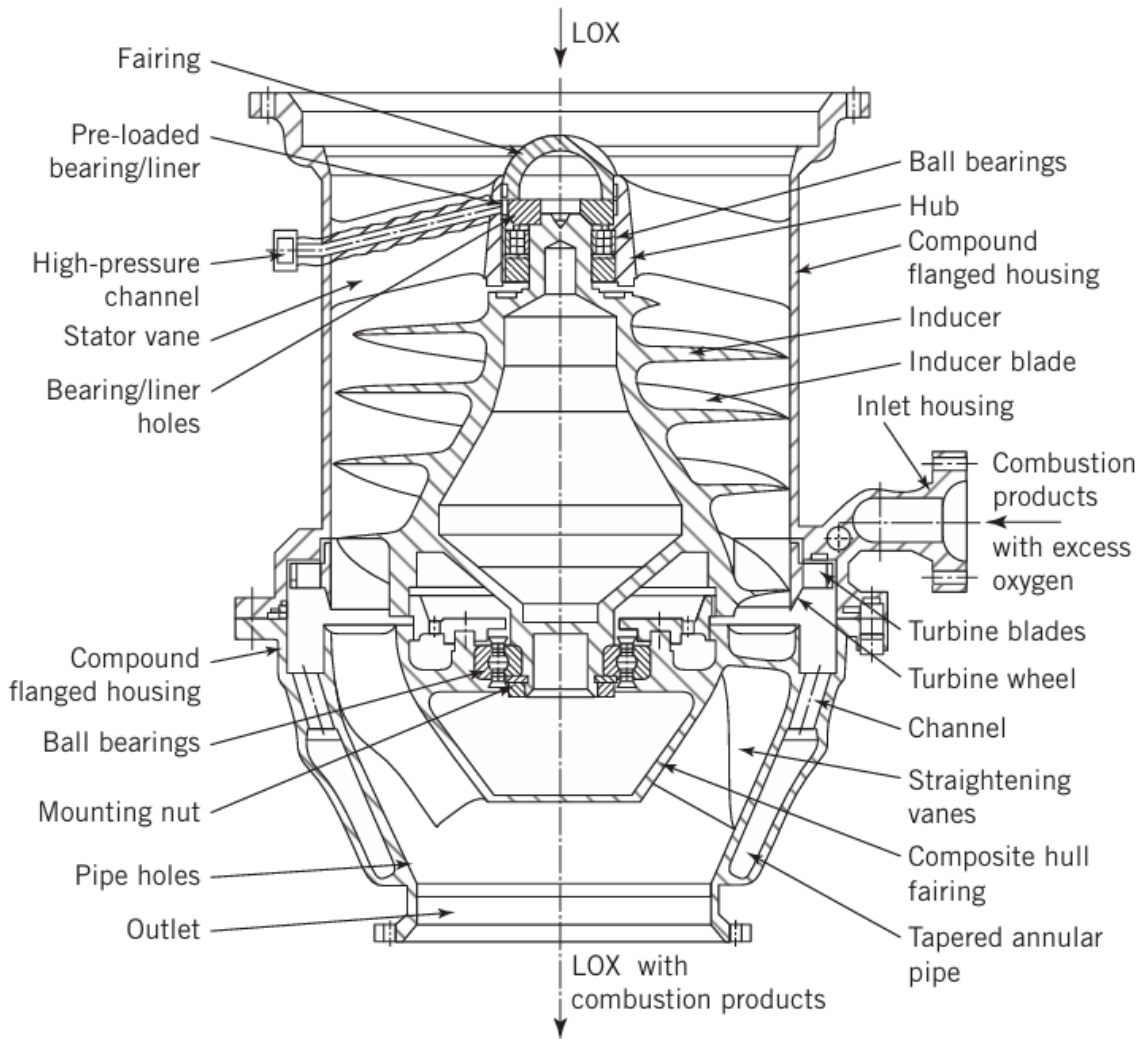
1. Crystal Structure: Titanium alloy Ti-6Al-4V has a hexagonal close-packed crystal structure.
2. Lattice Parameters: $a = 2.95$ Å, $c = 4.69$ Å (lattice parameters for titanium).
3. Density: 4.5 g/cm³ (density of titanium).

Spacecraft Specifications

1. Mass: 3625 kg (approximately 7992 pounds).
2. Dimensions: Diameter of 3.5 meters (11.5 feet), height of 2.7 meters (8.9 feet).
3. Orbit: Polar orbit around Jupiter, with a periapsis of approximately 4200 km (2600 miles) and an apoapsis of approximately 8.1 million km (5 million miles).

Electronic Components

1. RAD750 Processor: Radiation-hardened processor that provides reliable processing in high-radiation environments.
2. Electronic Boxes: At least 20 different electronic boxes, each with its own specific function and design.
3. Power and Data Distribution: Power and data distribution unit that provides power and data to the various electronic components.



Metrics and Materials/Components

Propulsion

- Main Engine:
- Type: Liquid fuel engine
- Thrust: 400 N (90 lbf)
- Fuel: Monomethylhydrazine and nitrogen tetroxide
- Fuel tank: Capacity of 925 kg (2039 lb)
- Propulsion System:
- Mass: 150 kg (331 lb)
- Length: 2.5 m (8.2 ft)
- Diameter: 1.5 m (4.9 ft)

Power Generation

- Power Generators:
- Type: Radioisotope thermoelectric generators (RTGs)
- Power: 570 watts

- Fuel: Plutonium-238
- Mass: 57 kg (125 lb)
- Batteries:
 - Type: Lithium-sulfur batteries
 - Capacity: 7.2 ampere-hours
 - Voltage: 28.05 volts
 - Mass: 13 kg (29 lb)

Communications

- High-Gain Antenna:
 - Type: Reflector antenna
 - Diameter: 4.2 m (13.8 ft)
 - Wavelength: 13 cm (5.1 in)
 - Gain: 37 dB
- Low-Gain Antenna:
 - Type: Omnidirectional antenna
 - Wavelength: 13 cm (5.1 in)
 - Gain: 10 dB

Scientific Instruments

- Camera:
 - Type: Solid-state camera
 - Resolution: 800x800 pixels
 - Wavelength: 400-1100 nm
 - Mass: 29.7 kg (65 lb)
- Near-Infrared Mapping Spectrometer:
 - Type: Mapping spectrometer
 - Wavelength: 0.7-5.2 micrometers
 - Resolution: 256x256 pixels
 - Mass: 18 kg (40 lb)

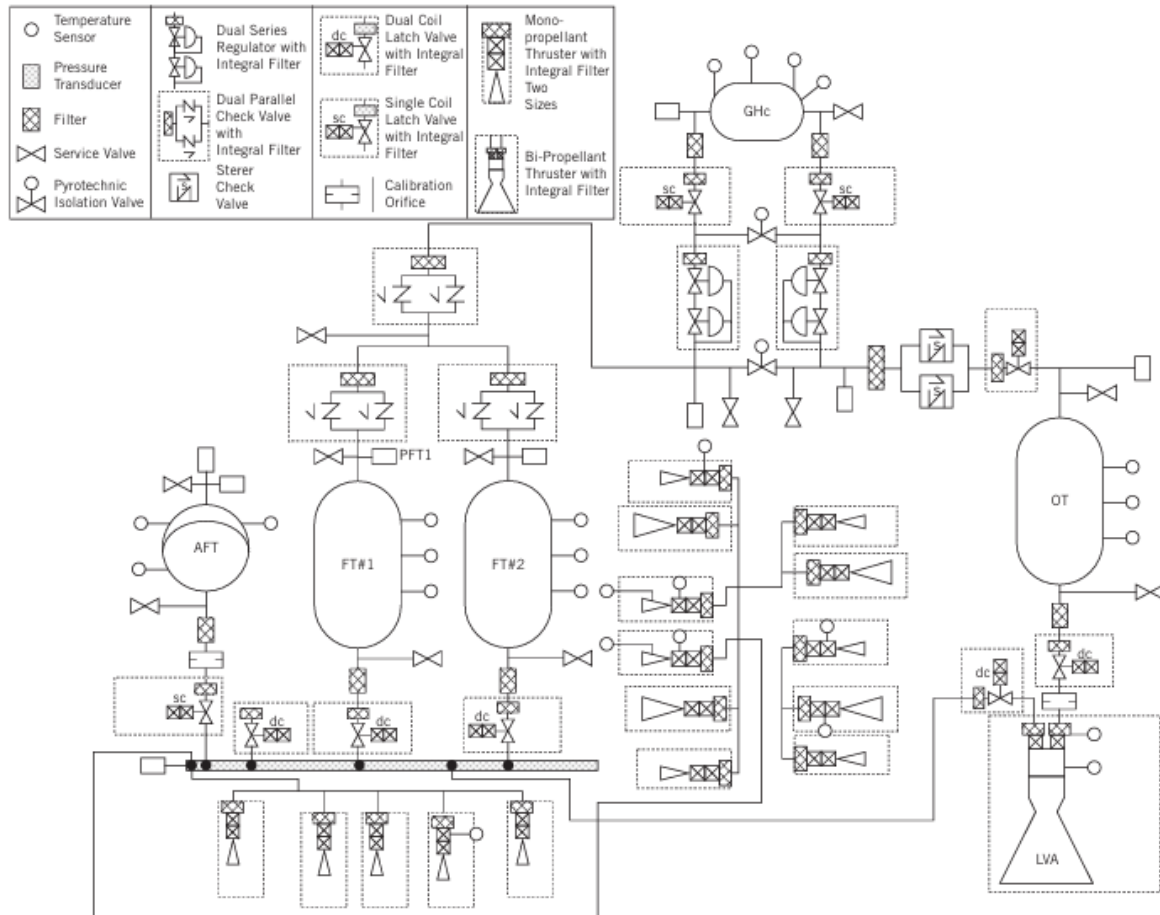
Black Hole Metrics

- Schwarzschild Mass:
 - Unit: kg
 - Value: 2.8×10^{30} kg (approximately 1.4 times the mass of the Sun)
- Schwarzschild Radius:
 - Unit: km
 - Value: 4.2×10^3 km (approximately 2.6 times the radius of the Sun)
- Surface Gravity:
 - Unit: m/s²
 - Value: 3.1×10^6 m/s² (approximately 300,000 times Earth's gravity)
- Binding Energy:
 - Unit: J
 - Value: 2.2×10^{41} J (approximately 100 times the energy released by the Sun in one second)

Materials and Components

- Titanium:
- Alloy: Ti-6Al-4V
- Properties: high strength, low density, corrosion resistance
- Copper:

- Properties: high electrical conductivity, high thermal conductivity
- Plutonium-238:
 - Properties: high specific energy, long half-life
- Lithium and Sulfur:
 - Properties: high energy density, long cycle life



Galileo Spacecraft Subsystems

Command and Data Handling (CDH)

- Subsystem Type: Actively redundant with two parallel data system buses
- Components:
 - Multiplexers (MUX)
 - High-level modules (HLM)
 - Low-level modules (LLM)
 - Power converters (PC)
 - Bulk memory (BUM)

- Data management subsystem bulk memory (DBUM)
- Timing chains (TC)
- Phase locked loops (PLL)
- Golay coders (GC)
- Hardware command decoders (HCD)
- Critical controllers (CRC)
- Functions:
 - Decoding of uplink commands
 - Execution of commands and sequences
 - Execution of system-level fault-protection responses
 - Collection, processing, and formatting of telemetry data for downlink transmission
- Movement of data between subsystems via a data system bus

Propulsion

- Subsystem Type: Propulsion module
- Components:
 - 400 N (90 lbf) main engine
 - Twelve 10 N (2.2 lbf) thrusters
 - Propellant, storage and pressurizing tanks
 - Associated plumbing
- Functions:
 - Propulsion for the spacecraft

Electrical Power

- Subsystem Type: Radioisotope thermoelectric generators (RTGs)
- Components:
 - Two RTGs
 - Plutonium-238 fuel
- Functions:
 - Generation of electricity for the spacecraft

Telecommunications

- Subsystem Type: High-gain antenna
- Components:
 - High-gain antenna
 - Low-gain antenna
- Functions:
 - Communication with Earth

Instruments

- Subsystem Type: Scientific instruments
- Components:
 - Solid-state imager (SSI)
 - Near-infrared mapping spectrometer (NIMS)
 - Ultraviolet spectrometer / extreme ultraviolet spectrometer (UVS/EUV)
 - Photopolarimeter-radiometer (PPR)
 - Dust-detector subsystem (DDS)
 - Energetic-particles detector (EPD)
 - Heavy-ion counter (HIC)
 - Magnetometer (MAG)

- Plasma subsystem (PLS)
- Plasma-wave subsystem (PWS)
- Functions:
- Study of Jupiter's atmosphere, magnetosphere, and moons

Deployable Structures

Types of Deployable Structures

- Folding: Deployable solar arrays, antennas
- Sleeve: Deployable antennas, radiators
- Truss: Deployable structures for large antennas, solar sails
- Inflatable: Deployable structures for solar sails, deorbit devices

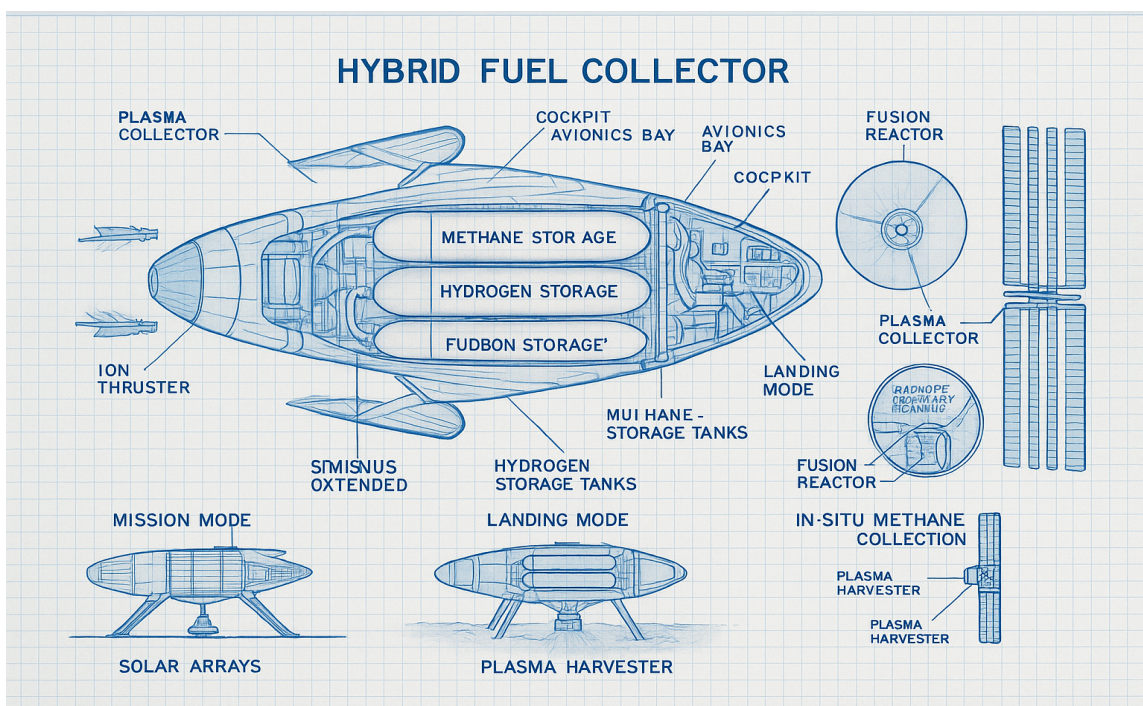
Examples of Deployable Structures

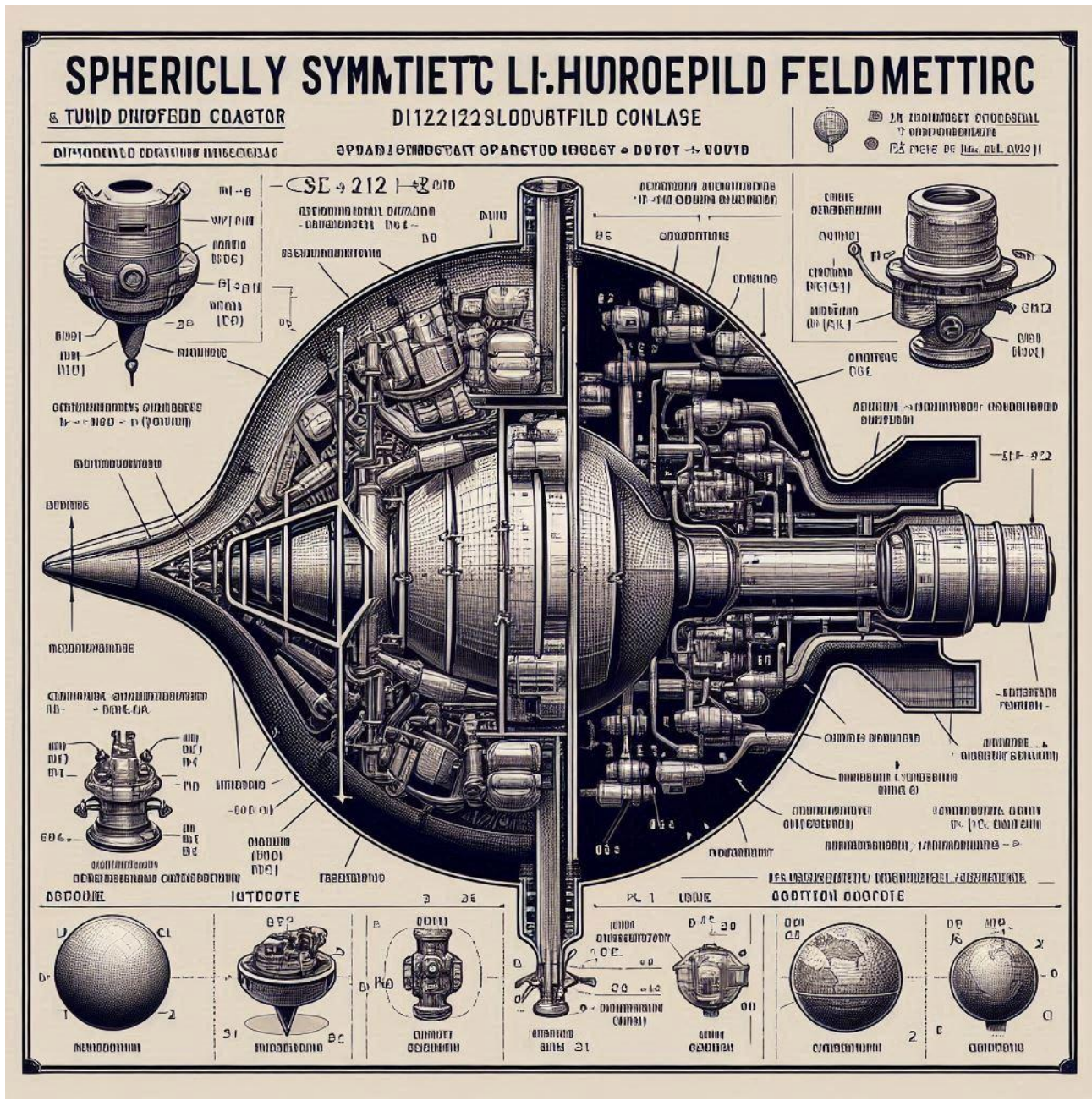
- GPX-2 CubeSat: Deployable boom for gravity gradient stabilization
- NASA Deployable Composite Booms (DCB): High bending and torsional stiffness, packaging efficiency, thermal stability, and 25% less weight than metallic booms
- Advanced Composite Solar Sail System (ACS3): Deployable boom technology for solar sailing applications

Metrics

Spacecraft Metrics

- Mass: 3625 kg (approximately 7992 pounds)
- Dimensions: Diameter of 3.5 meters (11.5 feet), height of 2.7 meters (8.9 feet)
- Orbit: Polar orbit around Jupiter, with a periapsis of approximately 4200 km (2600 miles) and an apoapsis of approximately 8.1 million km (5 million miles)



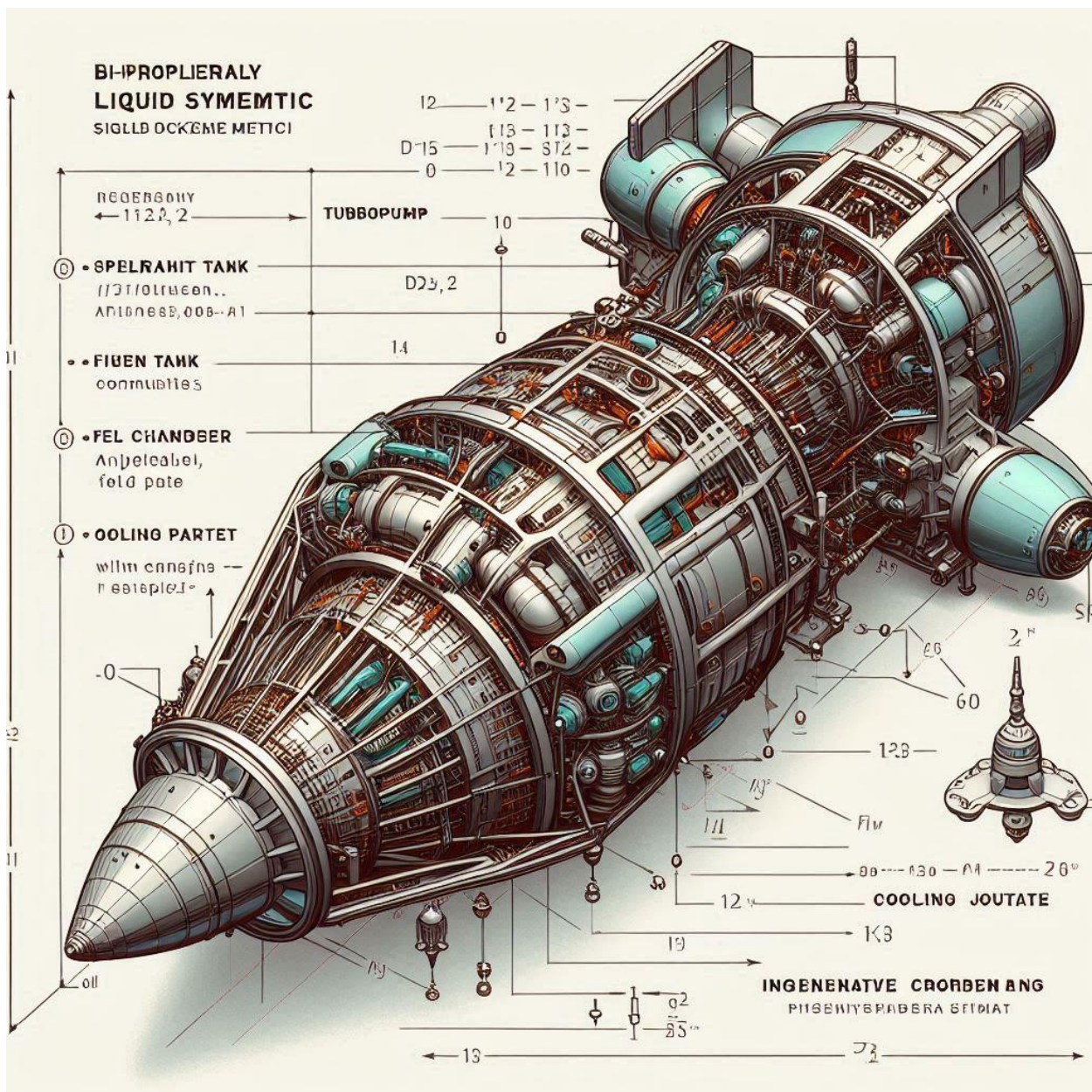


Instrument Metrics(VARIABLES)

- Solid-state imager (SSI):
- Mass: 29.7 kg (65 pounds)
- Power consumption: 15 watts
- Spectral response: 400 to 1100 nm
- Near-infrared mapping spectrometer (NIMS):
- Mass: 18 kg (40 pounds)
- Power consumption: 12 watts
- Spectral response: 0.7 to 5.2 micrometers

Deployable Structure Metrics

- GPX-2 CubeSat deployable boom:
 - Length: 2 meters (6.6 feet)
 - Mass: 4 kg (8.8 pounds)
 - NASA Deployable Composite Booms (DCB):
 - Length: up to 16.5 meters (54 feet)
 - Mass: 25% less than metallic booms



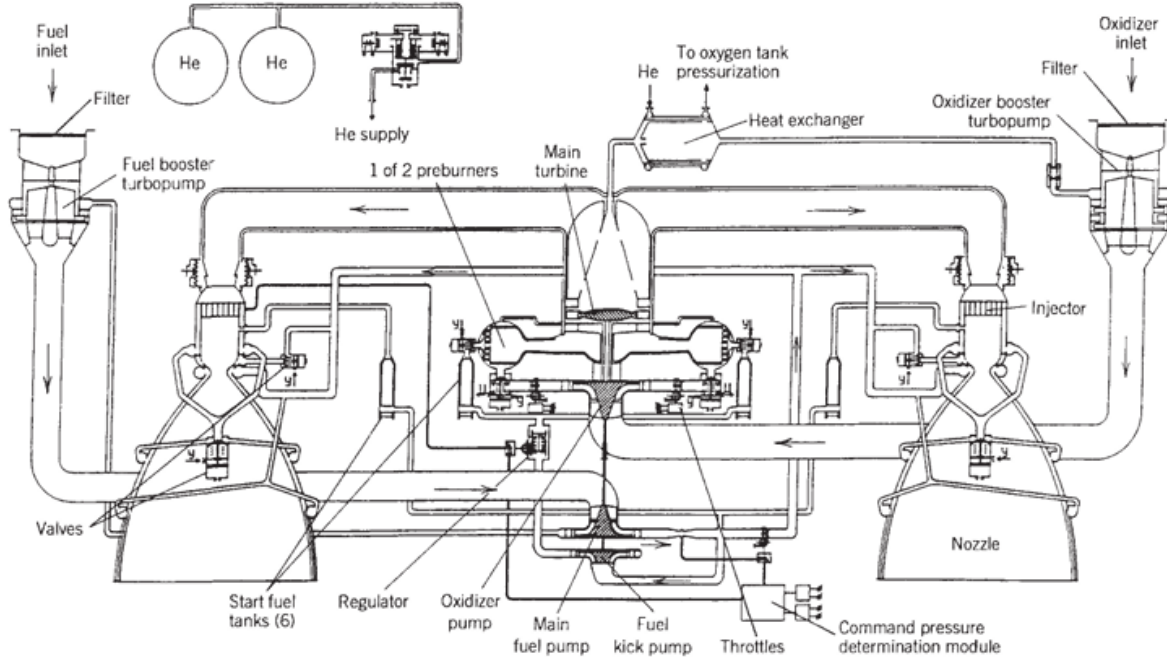


FIGURE 11–2. Simplified flow diagram of the RD-170 high-pressure rocket engine. The single-shaft large turbopump has a single-stage reaction turbine, two fuel pumps, and a single-stage oxygen pump with an inducer impeller. All of the oxygen and a small portion of the fuel flow supply two preburners. The oxidizer-rich gas drives the turbine, then entering the four thrust chamber injectors (only two are shown). The two booster pumps prevent cavitation in the main pumps. The pressurized helium subsystem (only partially shown) supplies various actuators and control valves; it is indicated by the symbol y . Ignition is accomplished by injecting a hypergolic fuel into the two preburners and the four thrust chambers. From NPO Energomash, Khimki, Russia, from Ref. 11–6.

The isentropic efficiency of the intake is denoted by (η_d) , which is static-to-total efficiency and is a measure for the losses from the far upstream conditions to the end of inlet (it is the fan/compressor face for turbine or shaft-based engines and the inlet of combustion chamber for ram-based engines). The efficiency is then expressed by the following relation (refer to Fig. 8.38):

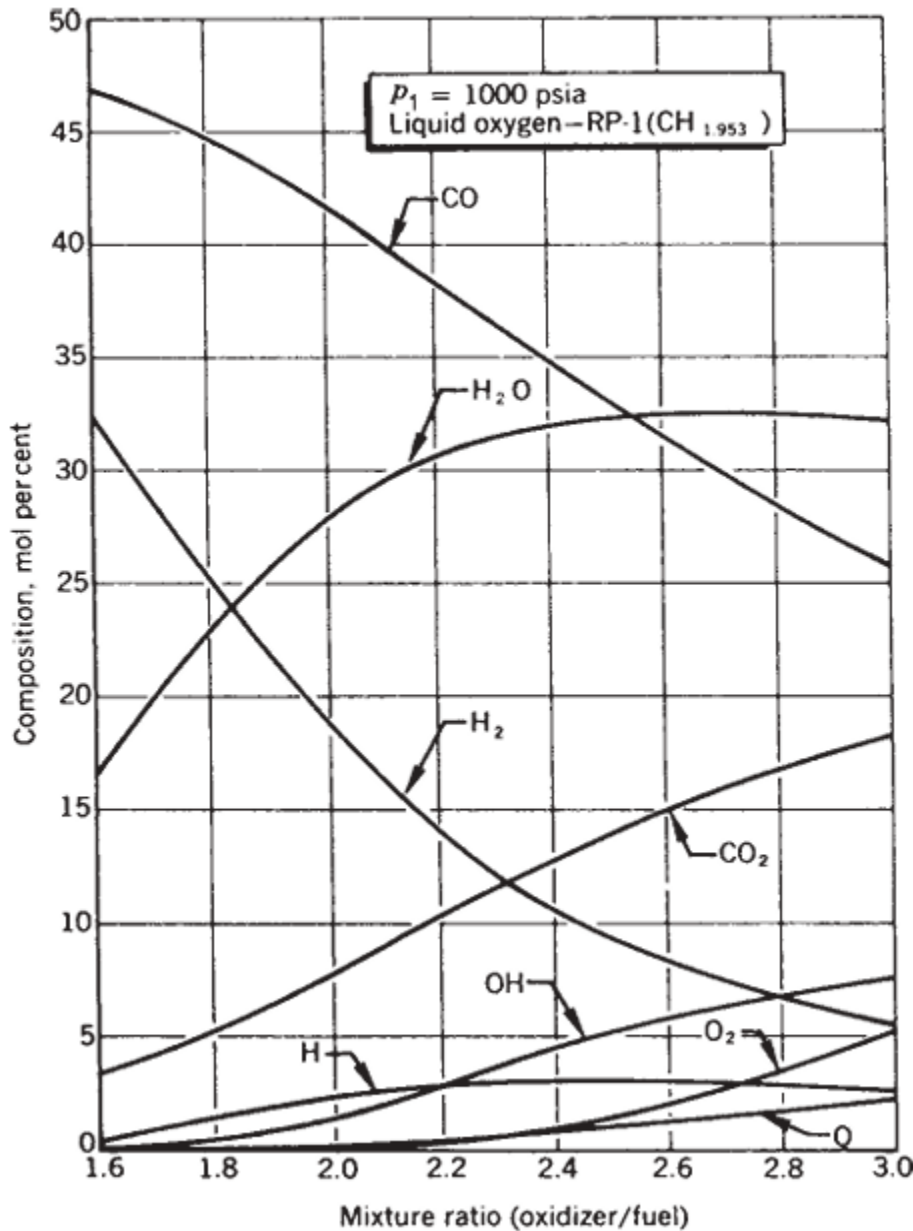
$$\begin{aligned}
 \eta_d &= (h_{02s} - h_1) / (h_{02} - h_1) \\
 &= (T_{02s} - T_1) / (T_{02} - T_1) \\
 &= (T_{02s}/T_1 - 1) / (T_{02}/T_1 - 1) \\
 \therefore \eta_d &= (rd)^{(\gamma-1)/\gamma} * [(1 + (\gamma-1)/2 * M_1^{<2}) / (1 + (\gamma-1)/2 * M_1^{<2})]
 \end{aligned}$$

(8.2) Stagnation pressure ratio is then expressed as

$$rd = p_{02} / p_{01} =$$

$$[1 + \eta d * (\gamma - 1) / 2 * M_1^2]^{(\gamma / (\gamma - 1))} /$$

$$[1 + (\gamma - 1) / 2 * M_1^2]^{(\gamma / (\gamma - 1))}$$



1. The working fluid (which usually consists of chemical reaction products) is homogeneous in composition.
2. All the species of the working fluid are treated as gaseous. Any condensed phases (liquid or solid) add a negligible amount to the total mass.

3. The working fluid obeys the perfect gas law.
4. There is no heat transfer across any and all gas-enclosure walls; therefore, the flow is adiabatic.
5. There is no appreciable wall friction and all boundary layer effects may be Neglected.
6. There are no shock waves or other discontinuities within the nozzle flow.
7. The propellant flow rate is steady and constant. The expansion of the working fluid is uniform and steady, without gas pulsations or significant turbulence.
8. Transient effects (i.e., start-up and shutdown) are of such short duration that they may be neglected.
9. All exhaust gases leaving the rocket nozzles travel with a velocity parallel to the nozzle axis.
10. The gas velocity, pressure, temperature, and density are all uniform across any section normal to the nozzle axis.
11. Chemical equilibrium is established within the preceding combustion chamber and gas composition does not change in the nozzle (i.e., frozen composition flow).
12. Ordinary propellants are stored at ambient temperatures. Cryogenic propellants are at their boiling points.

$$h_0 = h + v^2 / (2J) = \text{constant}$$

Conservation of energy applied to isentropic flows between any two nozzle axial sections x and y shows that the decrease in static enthalpy (or thermodynamic content of the flow) appears as an increase of kinetic energy since any changes in potential energy may be neglected.

$$hx - hy = (1/2) * (vy^2 - vx^2) / J = cp * (Tx - Ty)$$

Specific volume V (i.e., the volume divided by the mass within), at any section:

$$\dot{m}_x = \dot{m}_y \equiv \dot{m} = A * v / V$$

$$px * V_x = R * T_x$$

$$T_0 = T + v^2 / (2 * cp * J) \quad (3-8)$$

Relationship of area ratio, pressure ratio, and temperature ratio as functions of Mach number in a converging/diverging nozzle depicted for the subsonic and supersonic nozzle regions.

The nozzle area ratio for isentropic flow may now be expressed in terms of Mach numbers for two arbitrary locations x and y within the nozzle. Such a relationship is plotted in Fig. 3-1 for $M_x = 1.0$, where $A_x =$ At the throat or minimum area, along with corresponding ratios for T/T_0 and p/p_0 . In general,

$$A_y / A_x = (M_x / M_y) * \sqrt{[1 + ((k-1)/2) * M_y^2] / [1 + ((k-1)/2) * M_x^2]}^{(k+1)/(k-1)}$$

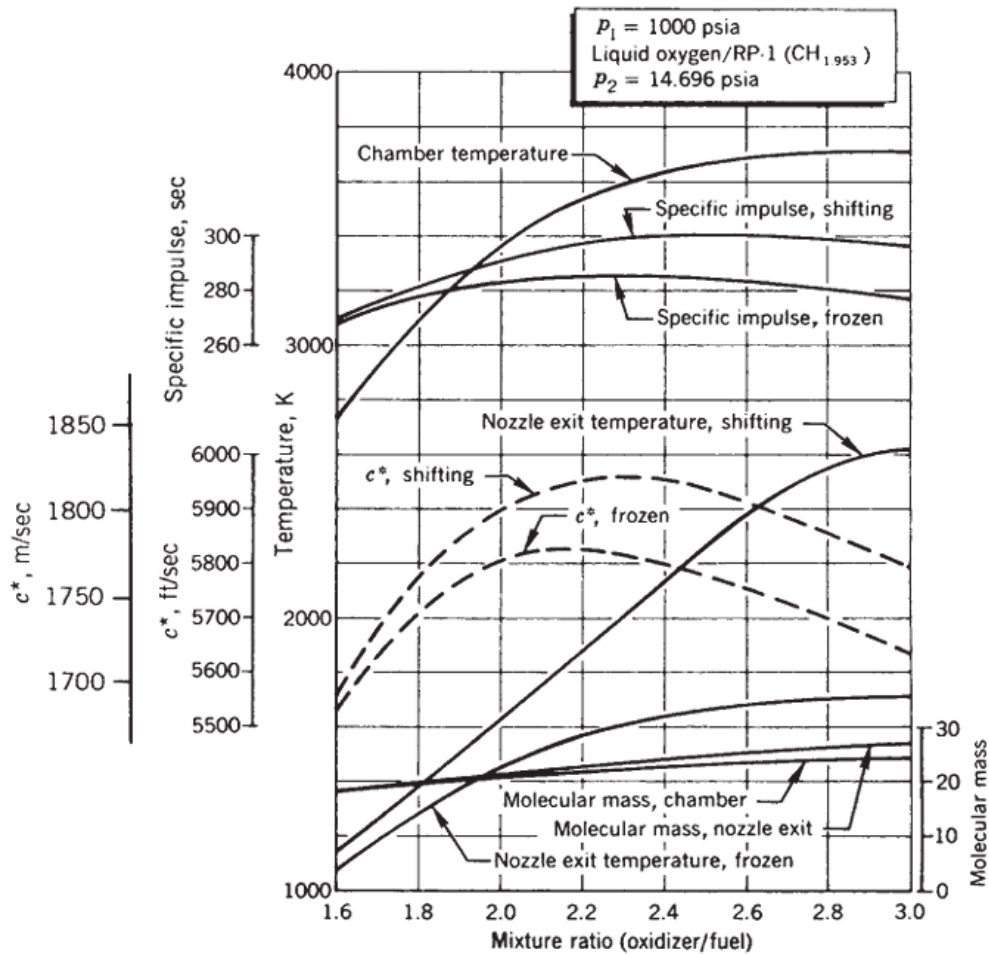


FIGURE 5-1. Calculated performance of liquid oxygen and hydrocarbon combustion as a function of mixture mass ratio.

temperature will be relatively low, the percentage of remaining O₂ and the percentage of the dissociation products (O, H, and OH) would all be very low and may be neglected. Thus, n_O , n_H , n_{OH} , and n_{O_2} are set to be zero. The solution requires knowledge of the enthalpy change of each of the species, and that information can be obtained from existing tables, such as Table 5–2 or Refs. 5–8 and 5–9.

In more general form, the mass for any given element must be the same before and after the reaction. The number of kg-mol of a given element per kilogram of reactants and product is equal, or their difference is zero. For each atomic species, such as the H or the O in Eq. 5–20,

$$\left[\sum_{j=1}^m a_{ij} n_j \right]_{\text{products}} - \left[\sum_{j=1}^r a_{ij} n_j \right]_{\text{reactants}} = 0 \quad (5-21)$$

Here, the atomic coefficients a_{ij} are the number of kilogram atoms of element i per kg-mol of species j , and m and r are indices as defined above. The average molecular mass for the products, using Eqs. 5–5 and 5–19, becomes

$$\bar{M} = \frac{2n_{H_2} + 32n_{O_2} + 18n_{H_2O} + 16n_O + n_H + 17n_{OH}}{n_{H_2} + n_{O_2} + n_{H_2O} + n_O + n_H + n_{OH}} \quad (5-22)$$

An "ideal rocket engine" is designed to operate at sea level using a propellant whose products of combustion have a specific heat ratio k of 1.3. Determine the required chamber pressure if the exit Mach number is 2.52. Also determine the nozzle area ratio between the throat and exit.

SOLUTION. For "optimum expansion" the nozzle exit pressure must equal the local atmospheric pressure, namely, 0.1013 MPa. If the chamber velocity may be neglected, then the ideal chamber pressure is the total stagnation pressure, which can be found from Eq. 3-13 as:

$$\begin{aligned} p_0 &= p * [1 + 1/2 * (k - 1) * M^2]^{(k / (k - 1))} \\ &= 0.1013 * [1 + 0.15 * (2.52)^2]^{(1.3 / 0.3)} \\ &= 1.84 \text{ MPa} \end{aligned}$$

The ideal nozzle area ratio A_2/A_1 is determined from Eq. 3-14 setting $M_t = 1.0$ at the throat

(see also Fig. 3-1):

$$\begin{aligned} A_2 / A_t &= (1 / M_2) * \\ &\quad [(1 + ((k - 1)/2) * M_2^2) / (k + 1)/2]^{[(k + 1) / (2 * (k - 1))]} \\ &= (1 / 2.52) * \\ &\quad [(1 + 0.15 * 2.52^2) / 1.15]^{(2.3 / 0.6)} \\ &= 3.02 \end{aligned}$$

Note that *ideal* implies no losses, whereas *optimum* is a separate concept reflecting the best calculated performance at a particular set of given pressures. Optimum performance is often taken as the design condition and it occurs when $p_2 = p_3$, as will be shown in the section on the thrust coefficient (the peak of the curves in Figs. 3-6 and 3-7 for fixed p_1/p_3).

The nozzle exit velocity (at $y = 2$), v_2 , can be solved for from Eq. 3-2:

$$v_2 = \sqrt{[2J(h_1 - h_2) + v_1^2]} \quad (3-15a)$$

As stated, this relation strictly applies when there are no heat losses. This equation also holds between any two locations within the nozzle, but hereafter subscripts 1 and 2 will only designate nozzle inlet and exit conditions.

For constant k , the above expression may be rewritten with the aid of Eqs. 3-6 and 3-7:

$$v_2 = \sqrt{[(2k / (k - 1)) * R * T_1 * [1 - (p_2 / p_1)^{((k - 1)/k)}] + v_1^2]}$$

A liquid oxygen–liquid hydrogen rocket thrust chamber that produces 10,000-lbf thrust, operates at a chamber pressure of 1000 psia, a mixture ratio of 3.40, has exhaust products with a mean molecular mass \bar{M} of 8.90 lbm/lb-mol, combustion temperature T_1 of 4380°F, and specific heat ratio of 1.26. Determine the nozzle throat area, nozzle exit area for optimum operation at an altitude where $p_3 = p_2 = 1.58$ psia, the propellant sea-level weight and the volume flow rates, and the total propellant requirements for 2.5 min of operation. For this problem, assume that the actual specific impulse I_s is 97% theoretical and that the thrust coefficient CF is 98% of the ideal value.

SOLUTION. The exhaust velocity for an optimum nozzle is determined from Eq. 3-16, but with a correction factor of g_0 for the English Engineering system:

$$c = v_2 = \sqrt{[2 g_0 k / (k - 1) * (R' T_1 / \bar{M}) * (1 - (p_2 / p_1)^{((k - 1)/k)})]}$$

$$= \sqrt{[2 \times 32.2 \times 1.26 / 0.26 \times 1544 \times 4840 / 8.9 \times (1 - 0.00158^0.206)]} = 13,890 \text{ ft/sec}$$

The theoretical specific impulse is $c/g_0 = 13,890 / 32.2 = 431$ sec. The actual specific impulse then becomes $0.97 \times 431 = 418$ sec.

The theoretical or ideal thrust coefficient is found from Eq. 3-30 or Fig. 3-5 ($p_2 = p_3$) for pressure ratio $p_1/p_2 = 633$ to be $CF = 1.76$. Actual thrust coefficient is 98% of this, so $CF = 1.72$.

The throat area required may be found from Eq. 3-31:

$$At = F / (CF p_1) = 10,000 / (1.72 \times 1000) = 5.80 \text{ in.}^2 \text{ (2.71 in. diameter)}$$

The optimum area ratio is found from Eq. 3-25 or Fig. 3-4 to be 42. The exit area is $5.80 \times 42 = 244 \text{ in.}^2$ (17.6 in. diameter).

At sea level, the weight density of oxygen is 71.1 lbf/ft³ and hydrogen 4.4 lbf/ft³.

Propellant weight flow rates (Eqs. 2-5, 6-3, and 6-4) at sea level are:

$$\dot{m}_w = F / I_s = 10,000 / 418 = 24.0 \text{ lbf/sec}$$

$$\dot{m}_{wo} = \dot{m}_w r / (r + 1) = 24.0 \times 3.40 / 4.40 = 18.55 \text{ lbf/sec}$$

$$\dot{m}_{wf} = \dot{m}_w / (r + 1) = 24 / 4.40 = 5.45 \text{ lbf/sec}$$

Volume flow rates from densities:

$$\tilde{V}_o = \dot{m}_{wo} / \rho_o = 18.55 / 71.1 = 0.261 \text{ ft}^3/\text{sec}$$

$$\tilde{V}_f = \dot{m}_{wf} / \rho_f = 5.45 / 4.4 = 1.24 \text{ ft}^3/\text{sec}$$

For 150 sec operation (including start/stop transients):

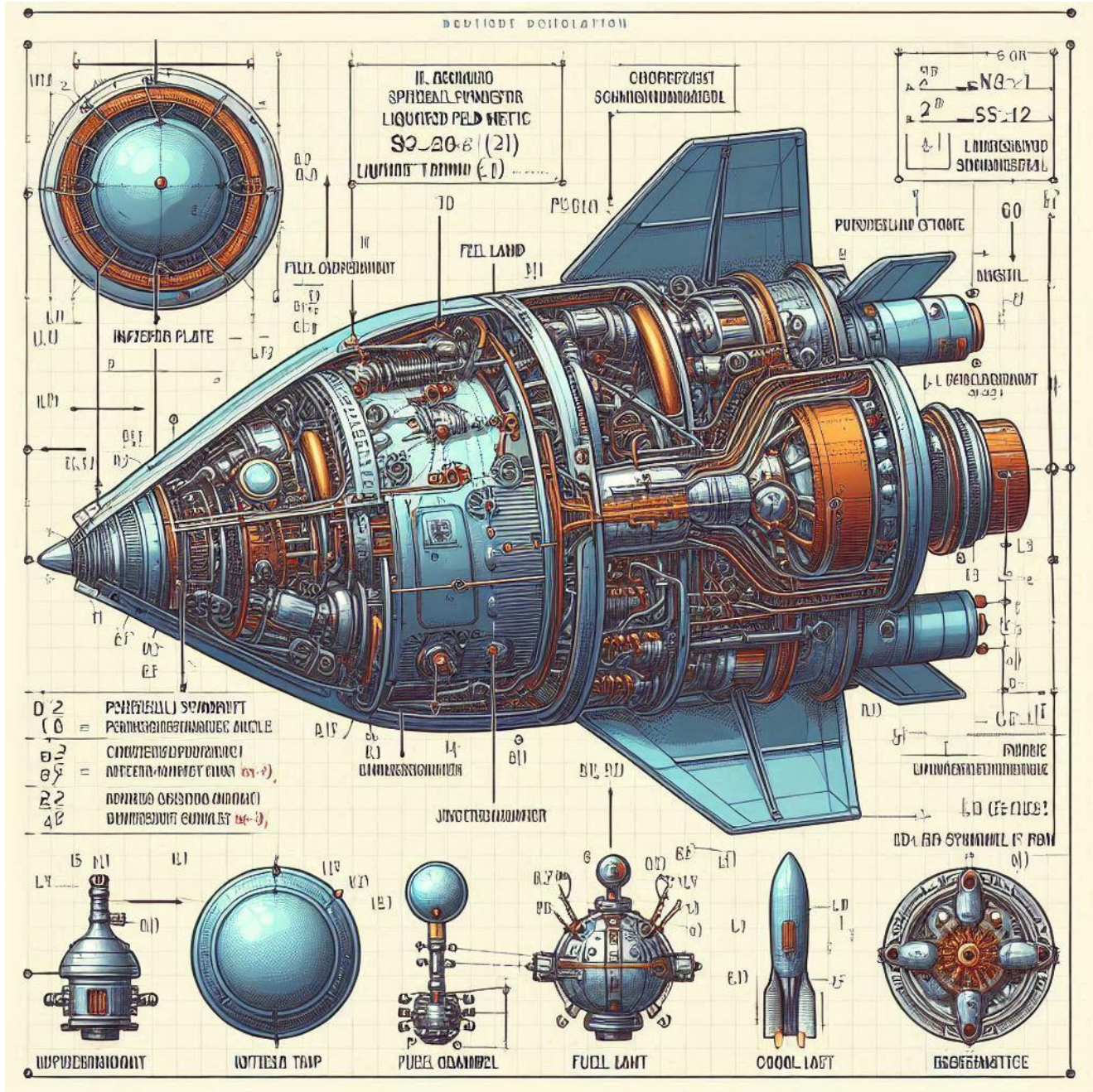
Oxygen weight: $18.55 \times 152 = 2820$ lbf

Hydrogen weight: $5.45 \times 152 = 828$ lbf

Oxygen volume: $0.261 \times 152 = 39.7 \text{ ft}^3$

Hydrogen volume: $1.24 \times 152 = 188.5 \text{ ft}^3$

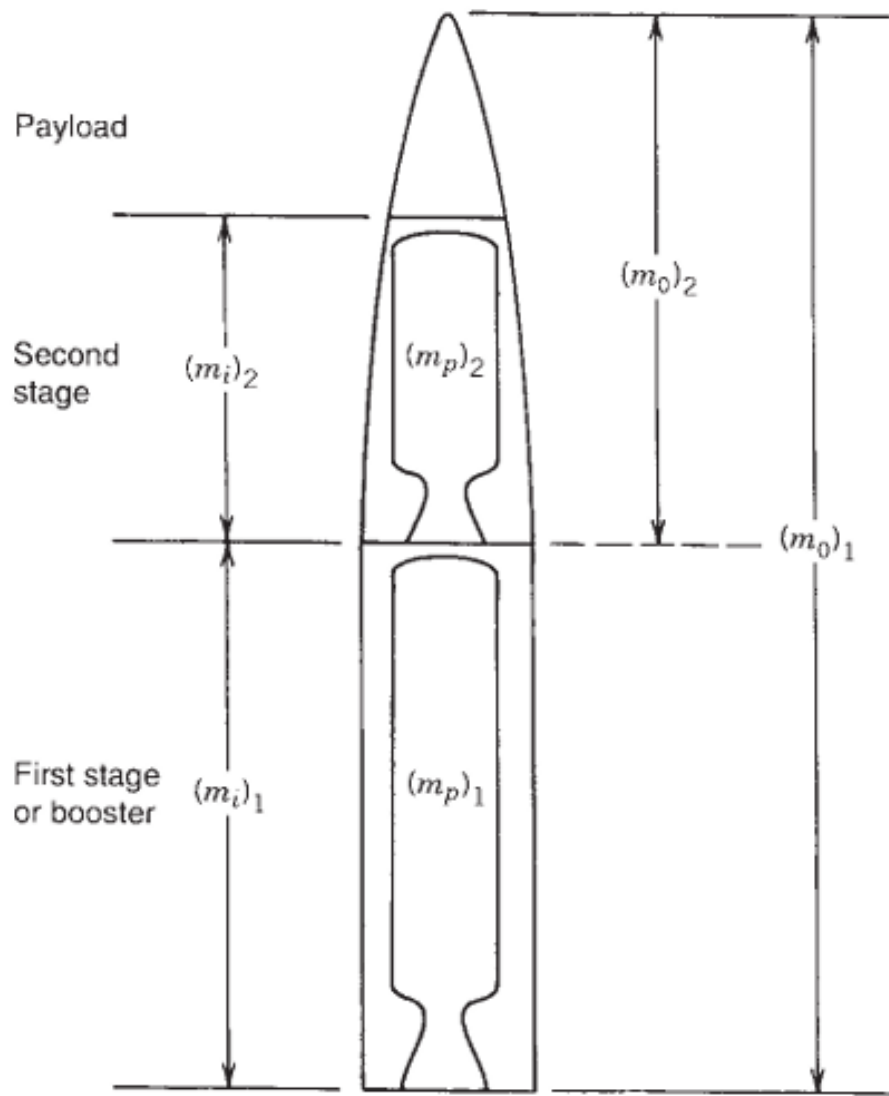
Note hydrogen volume is nearly five times oxygen due to low density.



Propellant Tanks:

- Liquid bipropellant systems store oxidizer and fuel in separate tanks.
 - Tanks must handle cryogenic temperatures and pressures.
 - Materials include aluminum, stainless steel, titanium, alloy steels, and fiber-reinforced plastics.
 - Ullage volume (3-10% tank volume) allows for thermal expansion and gas accumulation.

- Expulsion efficiency is typically 97-99.7%, residual propellant remains in tanks and pipes.
- Optimal tank shape is spherical for minimum mass; larger tanks are often cylindrical.
- Cryogenic tanks are insulated, vented, and require pre-cooling to prevent ice formation.
- Pressure safety devices prevent overpressure and tank failure.
- Tanks operate at pressures from 1.3 to 9 MPa (200 to 1800 psi).



Liquid Propellant Rocket Propulsion Systems Main Components

Liquid propellant rocket propulsion systems include:

A rocket engine

A set of tanks to store and supply propellants

These systems contain all the necessary hardware and propellants to generate thrust.

Rocket Engine Structure & each engine consists of:

One or more thrust chambers, Feed mechanisms to deliver propellants from tanks to the chamber(s)

A power source to operate the feed mechanisms, Plumbing to transfer liquid propellants under pressure

A structural frame to transmit thrust forces

Control devices (e.g., valves) to:

Start/stop the engine

Vary propellant flow and thus adjust thrust

Propellant Delivery

There are two main delivery methods:

Pressurized gas expels the propellants from the tanks, Pumps transport propellants to the thrust chambers

In this example: Space Shuttle Main Engine (SSME) / RS-25

Thrust: 512,000 lbf (vacuum)

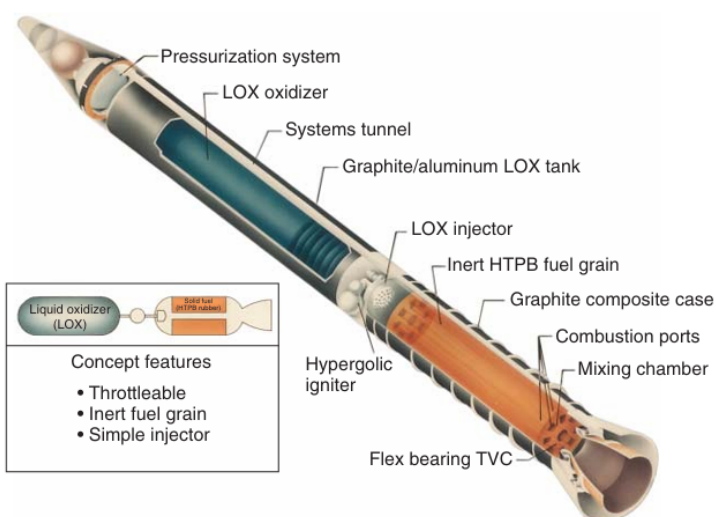


FIGURE 16–1. Depiction of a hybrid rocket preliminary concept aimed at boosting a large space vehicle. It has an inert solid fuel grain, pressurized liquid oxygen feed system, and can be throttled. Multiple ports are required to achieve the substantial fuel surface necessary for high flow rates.

Propellants: Liquid oxygen (LOX) and liquid hydrogen (LH₂)

RS-25 is a non-reusable version of the SSME with higher thrust

Includes:

2 low-pressure booster turbopumps

2 high-pressure main turbopumps, Tank pressurization via gasified LOX and LH₂

Additional Systems (in some engines) Thrust vector control (TVC) – for changing thrust direction

Thrust modulation – for variable thrust & the Engine condition monitoring – for engine health tracking.

Design Considerations

The propulsion system is tailored to specific mission requirements, such as:

Application (e.g., anti-aircraft missile, space launcher)

- 1) Flight path, velocity change, maneuvers
- 2) Storage/orbital life, number of units, safety, cost
- 3) From these mission requirements, engine specs are derived:
 - 1) Thrust-time profile
 - 2) Specific impulse

Number of chambers

- 1) Total impulse
- 2) Restart capability
- 3) Propellant choice
- 4) Engine mass and size
- 5) Optimization may apply to:
- 6) Thrust

7) Chamber pressure

Mixture ratio

Nozzle area

Component layout and cycles

Engine Classification

Engines can be:

Reusable (e.g., SSME)

Single-use (e.g., expendable launch vehicles)

Restartable or single-firing

Grouped by:

- Stage (booster/upper stage)
- Application
- Thrust level

Feed system type (pressurized vs turbopump)

Thrust Chamber

Main functions:

Mix, atomize, and burn propellants to produce high-speed exhaust

Major parts:

- Injector
- Combustion chamber
- Nozzle

1) Cooling methods:

Regenerative cooling - fuel circulates through walls to absorb heat

Radiation cooling - uses high-temp materials like niobium

Ablative cooling - materials absorb and vaporize heat

2) Feed Systems

Pump-fed systems - used for high-thrust applications

Pressure-fed systems – gas expels propellant from tanks

(Discussed in Sections 6.3, 6.4, 6.6)

Propellant Types
(Explained in Chapter 7)

Oxidizers: liquid oxygen, nitric acid, nitrogen tetroxide

Fuels: kerosene, alcohol, liquid hydrogen

Table 6-1: Engine Categories Summary rewritten in a linear and ordered format for clarity and study:

Engine Categories – Linear Comparison
1. Mission

Boost Propulsion: Large velocity change

Auxiliary Propulsion: Attitude/trajectory control

2. Applications

Boost Propulsion: Launch vehicles, missiles

Auxiliary Propulsion: Satellites, rendezvous stages

“Impulse & Boost Propulsion: High”

Auxiliary Propulsion: Low”

Number of Thrust Chambers, Boost Propulsion: 1–4”

Auxiliary Propulsion: 4–24, Thrust per Chamber

Boost Propulsion: 1,000–1,770,000 lbf & the Auxiliary Propulsion: 0.001–4,500 N (up to 1,000 lbf)

6. Feed System”

Boost Propulsion: Turbopumps (mostly)

Auxiliary Propulsion: Pressurized gas

7. Tank Pressure”

Boost Propulsion: 20–55 psi (0.14–0.38 MPa)

Auxiliary Propulsion: 100–2,500 psi (0.69–17.2 MPa)

8. Cooling Method & Boost Propulsion: Propellant-cooled

Auxiliary Propulsion: Radiation-cooled

9. Propellants Used

Boost Propulsion: Cryogenic or storable liquids”

Auxiliary Propulsion: Storable liquids, monopropellants

10. Chamber Pressure

Boost Propulsion: 350–3,600 psi (2.4–21 MPa)

Auxiliary Propulsion: 20–400 psi (0.14–2.1 MPa)

11. Number of Starts

Boost Propulsion: Up to 4”

Auxiliary Propulsion: Several thousand

12. Firing Duration

Boost Propulsion: A few minutes”

Auxiliary Propulsion: Up to several hours”

13. Shortest Possible Duration

Boost Propulsion: 5–40 seconds

Auxiliary Propulsion: Approximately 0.02 seconds (pulsing)

14. Start Time

Boost Propulsion: Up to several seconds

Auxiliary Propulsion: 0.004–0.080 seconds”

15. Operational Space Life

Boost Propulsion: Hours to months”

High-Pressure Gas Tanks:

Tanks for high-pressure gases used to push propellants need very high pressures (about 6.9 to 69 MPa or 1000 to 10,000 psi). These tanks are usually spherical to keep their weight low, and several small tanks can be linked together. Sometimes, small high-pressure tanks are placed inside the liquid propellant tanks.

Turbopump Feed Systems:

These systems pressurize the propellant tanks slightly (around 0.07 to 0.34 MPa or 10 to 50 psi) to prevent pump damage. The low pressure means tank walls can be thinner and lighter.

Problems in Flight: Liquids inside tanks can slosh around due to vehicle movements, causing issues like gas bubbles entering fuel lines, which can disrupt engine combustion. Vortexing (swirling) can also cause gas to enter outlets, especially if the vehicle spins. Internal baffles and special devices help reduce sloshing and vortexing. In zero gravity (space), liquids float and may not cover the tank outlet, allowing gas bubbles to enter. Special devices like pistons, bladders, flexible diaphragms, or surface tension screens help keep liquid at the outlet and prevent gas entry. Sometimes small thrusters apply acceleration to help settle the liquid in zero gravity.

Positive Expulsion Devices:

These devices separate pressurizing gas from liquid propellant to avoid mixing. Benefits include preventing gas dissolving in the propellant, allowing hot gases for pressurization, and avoiding chemical reactions or freezing in lines.

Different types include elastomeric diaphragms, inflatable bladders, metallic diaphragms, pistons, and surface tension screens, each with pros and cons.

Center of Gravity Control:

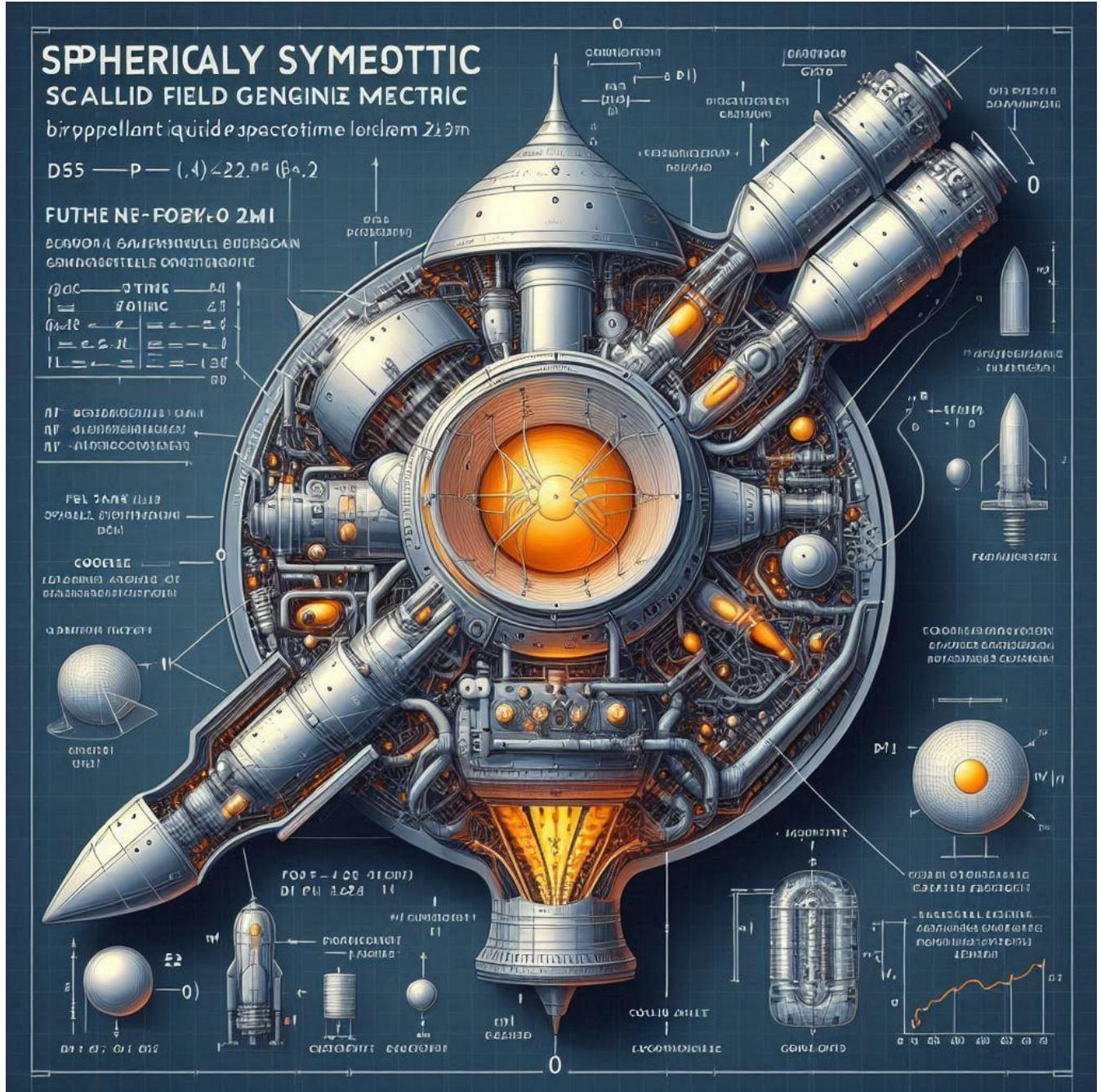
Piston devices help keep the vehicle's center of gravity predictable, important for stable flight and control.

Propellant Feed Systems Overview:

Their main jobs are to increase propellant pressure and deliver the right flow to the engines. Energy comes from pressurized gas, pumps, or both. The system design depends on mission needs, cost, complexity, and minimizing weight. Gas pressure feed systems work better for low total impulse and thrust, while turbopumps are better for high pressure and large missions.

Importance of Pressure and Flow

Knowing local pressures and flow rates is critical for design, testing, and engine control. It helps ensure engines run correctly, avoid damage, and optimize performance. Monitoring these values during tests can detect problems early.



Common Physical Hazards of Propellants

Corrosion: Certain propellants (e.g., nitrogen tetroxide, nitric acid, nitric oxide, hydrogen peroxide) require special container materials. Contamination with corrosion products can alter propellant properties, rendering them unsuitable. Corrosion from gaseous reaction products poses risks to launch structures and nearby communities.

Explosion Hazard: Some propellants (e.g., hydrogen peroxide, nitromethane) can destabilize over time and potentially detonate depending on impurities, temperature, and shock. Accidental mixing of liquid oxidizers (e.g., liquid oxygen) and fuels may cause detonations, often during transport or launch mishaps.

Fire Hazard: Many oxidizers react spontaneously with organics causing fires. Propellants like nitric acid, nitrogen tetroxide, fluorine, and hydrogen peroxide can ignite organic materials upon contact. Oxygen enhances existing fires but typically does not ignite materials alone.

Accidental Spills: Mishaps during engine operation or transport can cause hazardous spills leading to fires or health hazards. Regulatory guidelines govern marking, containment, and emergency responses.

Health Hazards: Exposure to many propellants causes toxic effects, including severe skin burns (e.g., nitric acid), nausea (aniline, hydrazine), carcinogenic risks (hydrazine derivatives), eye irritation, and respiratory damage from inhalation. OSHA limits define safe exposure thresholds.

Toxic Propellants Handling: Requires strict procedures for handling, transfer, transport, inspection, and post-test clean-up. Detection instruments, protective equipment (masks, gloves, shields), decontamination chemicals, and emergency protocols are essential. Toxic propellant operations demand significantly more trained personnel.

Materials Compatibility: Limited materials are compatible with certain propellants, especially for seals (gaskets, O-rings). Incompatible materials can cause leaks, fires, corrosion, or failure. Cryogenic propellants can make materials brittle; some materials catalyze decomposition (e.g., hydrogen peroxide).

Desirable Physical Properties:

Low Freezing Point to allow cold environment operation. The High Specific Gravity improves propellant mass per tank volume, reducing tank size and vehicle mass, positively impacting flight performance. Equations relate average specific gravity/density of bipropellant mixtures to fuel and oxidizer properties. Increasing propellant density increases mass flow and thrust. Cryogenic propellants (like LOX) have variable properties with temperature affecting performance.

Stability: Propellants must not chemically decompose during storage/operation, even at elevated temperatures. Should be chemically inert with system materials and resist moisture or impurities. Deposits from coolant decomposition can reduce heat transfer and cause failures.

Heat Transfer and Pumping Properties: High specific heat and thermal conductivity, low freezing point, and high boiling points are desirable for cooling. Low vapor pressures ease handling and pump design, reducing cavitation risk. High vapor pressure propellants require special materials and handling.

Temperature Variation Effects: Physical properties (density, viscosity, vapor pressure) should vary minimally and similarly for fuel and oxidizer to ensure consistent engine calibration and performance. Temperature mismatches can alter mixture ratios and produce unwanted residues.

Ignition and Combustion:

- Hypergolic Propellants ignite spontaneously on contact, simplifying ignition systems and reducing explosion risks.
- Non-hypergolic propellants require igniters for initial combustion energy, which should be minimal.
- Ignition delays increase at low temperatures.
- Combustion stability varies between propellant combinations, affecting desirability.
- Smoke and luminous exhaust may be problematic in military or sensitive applications due to detectability or interference.

Consistency: Propellant batches must maintain consistent physical and chemical properties to ensure predictable engine performance.

The most energetic known liquid oxidizer, producing the highest specific impulse and density, is liquid fluorine. Despite testing in experimental engines, it was abandoned due to extreme hazards. Other storable and cryogenic liquid oxidizers include mixtures of liquid oxygen and fluorine, oxygen difluoride (OF₂), chlorine trifluoride (ClF₃), and chlorine pentafluoride (ClF₅), but none are currently used because of their toxicity and corrosiveness.

Liquid Oxygen (LOX)

Widely used as an oxidizer, LOX burns with a bright white-yellow flame with most hydrocarbon fuels and hydrogen. It is common in large rocket engines, e.g., Atlas V, Soyuz, Ariane V, and Delta IV. LOX supports and accelerates combustion, but is noncorrosive and nontoxic if containers are clean. Handling requires insulation to minimize evaporation losses and avoid frostbite. LOX evaporates quickly and is typically produced near its point of use by fractional distillation of liquid air. Pressurization before engine start keeps LOX cold and dense.

Hydrogen Peroxide (H₂O₂)

Used in highly concentrated form (70–98%), known as High-Test Peroxide (HTP). It decomposes catalytically into steam and oxygen, yielding a theoretical monopropellant Isp ~154 sec. It is hypergolic with hydrazine and burns well with kerosene as bipropellant. H₂O₂ is highly reactive and causes severe burns. Storage stability has improved with better materials and cleaning, extending shelf life from 3–4 years to 12–16 years. Usage declined due to decomposition and handling difficulties but recent advances renewed interest.

Nitric Acid (HNO₃)

Various nitric acid mixtures, notably Red Fuming Nitric Acid (RFNA), were used between 1940–1965. RFNA contains dissolved nitrogen dioxide (5–27%) and is more energetic and stable than white fuming

nitric acid. Storage requires special materials like stainless steel or gold. Inhibited RFNA (IRFNA) with fluoride ions reduces corrosion. Nitric acid reacts violently with many fuels and organic materials, causing spontaneous ignition. It is highly corrosive and toxic; vapor exposure limits are strict.

Nitrogen Tetroxide (N₂O₄) – NTO

Common storable oxidizer, hypergolic with hydrazine and derivatives (MMH, UDMH). Yellow-brown liquid, specific gravity ~1.44. Mildly corrosive when pure, forms strong acids in presence of moisture. Highly toxic NO₂ fumes upon decomposition. Requires sealed heavy tanks due to high vapor pressure. Freezing point can be lowered by mixing with nitric oxide (NO) to form Mixed Oxides of Nitrogen (MON). Used in Russian engines, Space Shuttle systems, and many spacecraft thrusters. OSHA exposure limit is 5 ppm NO₂.

Nitrous Oxide (N₂O)

Known as “laughing gas,” used medically as anesthetic. Less potent oxidizer, supports combustion only at elevated temperatures. Much less toxic than N₂O₄, with a higher exposure limit. Decomposes into O₂ and N₂ with catalysts.

Python.

1. Liquid Oxygen (O₂)

Molecule: O₂

Function: Provides oxygen to burn the fuel (like hydrogen or kerosene).

Molecular process:

O₂ has a strong double bond but can split into two reactive oxygen atoms (O[·]).

These oxygen atoms react with fuel molecules, for example hydrogen (H₂), to form water (H₂O):



Oxygen gains electrons (is reduced), hydrogen loses electrons (oxidized), releasing energy.

Outcome: Energy release generates thrust.

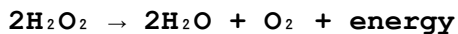
2. Hydrogen Peroxide (H₂O₂)

Molecule: H₂O₂

Function: Can act as oxidizer or monopropellant by decomposing to oxygen and steam.

Molecular process:

The O-O bond in H₂O₂ is weak and breaks in the presence of a catalyst (e.g., platinum):



Produces water vapor and oxygen gas.

Released oxygen supports combustion or the hot gas expansion creates thrust alone.

Outcome: Produces oxygen and steam to push the engine.

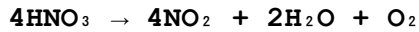
3. Nitric Acid (HNO₃) and Red Fuming Nitric Acid (RFNA)

Molecule: HNO₃

Function: Acts as an oxidizer releasing oxygen and reactive nitrogen oxides.

Molecular process:

Nitric acid decomposes to nitrogen dioxide (NO₂), water, and oxygen:



NO₂ is reactive and helps oxidize the fuel.

This can cause spontaneous ignition with certain fuels.

Outcome: Releases oxygen and NO₂ to oxidize fuel and release energy.

4. Dinitrogen Tetroxide (N₂O₄) / Nitrogen Dioxide (NO₂)

Molecule: N₂O₄

Function: Strong oxidizer, dissociates into two NO₂ molecules.

Molecular process:

Exists in equilibrium:



NO₂ reacts spontaneously with fuels like hydrazine, igniting without external spark:



NO_2 oxidizes nitrogen and hydrogen bonds in the fuel releasing heat.

Outcome: Instantaneous and hypergolic combustion.

5. Nitrous Oxide (N_2O)

Molecule: N_2O

Function: Weaker oxidizer, not flammable but supports combustion at high temperature.

Molecular process:

At high temperatures, decomposes into nitrogen (N_2) and oxygen (O_2):



Oxygen released supports burning of the fuel.

Outcome: Controlled oxygen release for combustion.

Summary of Molecular Behavior:

- O_2 splits into reactive oxygen atoms, burning fuel and releasing energy.
- H_2O_2 's O–O bond breaks with a catalyst, producing steam and oxygen for thrust.
- HNO_3 decomposes to NO_2 and O_2 , with NO_2 oxidizing fuel and possibly causing ignition.
- N_2O_4 exists in equilibrium with NO_2 ; NO_2 causes hypergolic combustion.
- N_2O decomposes thermally to release oxygen that sustains combustion.

6. Safety and Environmental Concerns To minimize hazards:

- Be aware of toxicity, explosiveness, fires, and spills.
- Personnel must receive specific safety training.
- Mandatory use of safety equipment: protective clothing, face shields, vapor detectors.
- Health monitoring for those exposed to toxic materials.

Rocket engine safety:

- Design to prevent leaks, spills, and fires.

- Safety reviews must be conducted during manufacturing and testing.
- Investigate unsafe practices and apply corrective actions.

Environmental concerns:

- Toxic exhaust and liquid spills contaminate air, water, soil.
- Regulated discharges require permits, with penalties for violations.
- Gelled propellants can reduce risks but are not widely adopted.

Conclusion:

With proper training, equipment, and design, propellant handling can be conducted safely.

7. Historical Engine Construction (Thor Missile Example)

- Early regeneratively cooled tubular thrust chamber.
- Fuel: Kerosene-type.
- Oxidizer: Liquid oxygen.
- Nozzle throat inside diameter: ~15 inches.
- Sea-level thrust progression:
120,000 → 135,000 → 150,000 → 165,000 lbf.
- Improvements by increasing flow, chamber pressure, and strengthening the hardware.
- Exit nozzle changed from cone-shaped to bell-shaped for efficiency.

SYMBOLS

a	burning or regression rate coefficient (units of a depend on value of oxidizer flux exponent)	variable units
A_p	combustion port area	m^2 (in. ²)
A_s	fuel grain surface area	m^2 (in. ²)
A_t	nozzle throat area	m^2 (ft ²)
c^*	characteristic velocity	m/sec (ft/sec)
C_{F_v}	vacuum thrust coefficient	dimensionless
c_p	heat capacity	J/kg-K (Btu/lbm-°R)
d_b	fuel grain burn distance	m (in.)
D_h	hydraulic diameter ($4A_p/P$)	m (in.)
D_p	combustion port diameter	m (in.)
D_t	nozzle throat diameter	m (in.)
F_v	vacuum thrust	N (lbf)
G	mass velocity	kg/m ² -sec (lbm/ft ² -sec)
G_o	oxidizer mass velocity	kg/m ² -sec (lbm/ft ² -sec)
g_0	acceleration of gravity—conversion factor	m/sec ² —32.174 lbm-ft/lbf-sec
h	convective heat transfer coefficient	J/m ² -sec/K (Btu/ft ² -sec/°R)
h_v	heat of gasification	J/kg (Btu/lbm)
Δh	flame zone-fuel surface enthalpy difference	J/kg (Btu/lbm)

INJECTORS

The various functions of fuel injectors are to introduce and meter liquid propellant flows into the combustion chamber, to break up liquid jets into small droplets (a process called atomization), and to distribute and mix the propellants so that the desired fuel and oxidizer mixture ratio results, with uniform propellant mass flow and composition across the chamber cross-section.

There are two common design approaches for delivering propellants into the combustion chamber. Older designs used a set of propellant jets that passed through a multitude of holes on the injector face. Many rocket injectors developed in the United States employed this type for both large and small thrust chambers. Various hole arrangements are shown in Figure 8–3.

The second design type uses individual cylindrical injection elements, which are inserted and fastened (welded, brazed, or soldered) into the injector face, and each element delivers a conically shaped spray of propellants into the combustion chamber. Figure 8–4 shows several common spray injection elements, producing conical propellant sheets either from slots or from the internal edges of a hollow cylinder within the element. This design has been widely used with liquid oxygen (LOX) and liquid hydrogen (LH_2) thrust chambers worldwide, including the Space Shuttle engines. It has also been the preferred approach in Russia, applied to most of their propellants and thrust chamber sizes. There are also other injector designs that combine jet and spray elements.

Injector face patterns are closely linked to the internal manifolds or feed passages. These distribute propellants from inlets to injection holes or spray elements. A large, complex manifold volume allows for low passage velocities and proper distribution across the chamber cross-section. Smaller manifold volumes lead to lighter injectors, faster ignition starts, and reduced "dribble" (the flow that occurs after the main valves close). However, higher passage velocities often cause uneven flow through identical injector holes, leading to poor distribution and large local composition variations. Upon thrust termination, any propellant dribble results in after-burning—an inefficient, irregular combustion effect that causes a small amount of residual thrust ("cutoff" thrust). For applications requiring precise final vehicle velocity, this cutoff impulse must be very small and repeatable; often, valves are built into injectors to minimize propellant passage volumes.

Doublet impinging-stream-type multiple-hole injectors are commonly used with oxygen–hydrocarbon and storable propellants, as shown in Figure 8–3. In "unlike" doublet patterns, fuel and oxidizer are injected through separate holes so that their streams impinge on one another. This impingement forms thin liquid fans, aiding in atomization and droplet distribution. Discharge coefficients for specific injector orifices are listed in Table 8–2.

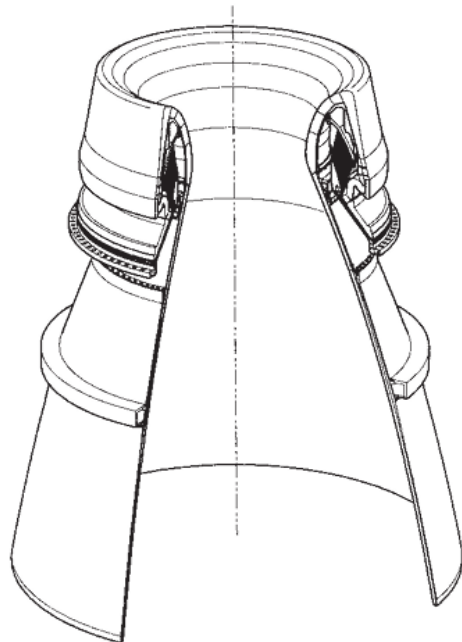
Imping-hole injectors can also use like-on-like or self-impinging patterns (e.g., fuel-on-fuel and oxidizer-on-oxidizer). In these, two liquid streams form a fan which then breaks into droplets. Unlike doublets, they work best when the volumetric flow of fuel and oxidizer is about equal and when ignition delays are long enough to allow fan formation. For uneven flow rates, triplet patterns tend to be more effective.

Non-impinging or showerhead injectors use propellant streams that emerge perpendicularly to the injector face. They rely on turbulence and diffusion to achieve mixing. The German V-2 rocket during World War II used this type of injector. However, these are no longer used, as they require relatively large chamber volumes for efficient combustion.

Sheet or spray-type injectors produce cylindrical, conical, and other types of spray sheets, which intersect to promote mixing and atomization. See Figure 8–4. The resulting droplets then vaporize. Droplet size distributions from spray injection elements are generally more uniform than those from impinging streams.

By adjusting internal dimensions of spray elements (such as the size or number of tangential feed holes, the length/protrusion of an internal cylinder, or the angle of an internal spiral rib), one can change the conical spray angle, the impingement location of fuel and oxidizer spray sheets, and affect mixture ratios, combustion efficiency, or stability. By varying the sheet widths (via an axially movable sleeve), it is possible to throttle propellant flows over a wide range without excessive reductions in injector pressure drop.

This type of variable-area concentric tube injector was used in the descent engine of the Apollo Lunar Excursion Module, where it was throttled over a 10:1 flow range with minimal effects on mixture ratio or performance.



RSRM Nozzle Characteristics

Type	Contoured or bell
Thrust vector control	Flexible bearing
Expansion area ratio	7.72
Throat diameter	53.86 in.
Exit diameter	149.64 in.
Total length	178.75 in.
Nozzle weight	23, 941 lbf
Maximum pressure	1.016 psi
Maximum thrust (vac.)	3, 070, 000 lbf
Burn time	123.7 sec
Materials	Steel and aluminum Carbon cloth phenolic
Housings	
Liners	

FIGURE 15–8. External quarter section view of nozzle configuration of the historic Space Shuttle reusable solid rocket motor (RSRM). Courtesy of Orbital ATK

PYTHON

```
-- INJECTOR FLOW CHARACTERISTICS --  
  
-- The injector plays a fundamental role in the design and operation of a  
rocket engine.  
  
-- AFFECTS:  
-- - atomization  
-- - combustion efficiency  
-- - heat transfer  
-- - transient behavior  
-- - stability  
  
-- DEPENDS ON:  
-- - propellants  
-- - injector geometry  
-- - thermodynamic and hydraulic characteristics  
  
-- MASS FLOW RATE:  
--  $\dot{m} = F / c$   
  
-- ORIFICE FLOW EQUATIONS:  
--  $Q = Cd * A * \sqrt{2 * \Delta p / \rho}$   
--  $\dot{m} = Cd * A * \sqrt{2 * \rho * \Delta p}$   
  
-- MIXTURE RATIO:  
--  $r = \dot{m}_o / \dot{m}_f$   
--  $= (Cd_o / Cd_f) * (A_o / A_f)$   
--  $* \sqrt{(\rho_o / \rho_f) * (\Delta p_o / \Delta p_f)}$   
  
-- INJECTION VELOCITY:  
--  $v = Q / A$   
--  $= Cd * \sqrt{2 * \Delta p / \rho}$   
  
-- MOMENTUM BALANCE / SHEET ANGLE:  
--  $\tan(\delta) = (\dot{m}_o * v_o * \sin(\gamma_o) - \dot{m}_f * v_f * \sin(\gamma_f)) /$   
--  $(\dot{m}_o * v_o * \cos(\gamma_o) + \dot{m}_f * v_f * \cos(\gamma_f))$   
  
-- ENGINEERING CONSIDERATIONS:  
-- -  $\Delta p$  is usually 20–30% of chamber pressure.  
-- - High  $\Delta p$  improves atomization but increases thermal load.  
-- - Injector spray angle affects wall impingement.  
-- - Symmetry and injector distribution affect stability and performance.  
*****  
*****  
-- ROCKET ENGINE COMBUSTION CHAMBER DATA --  
  
-- GIVEN PARAMETERS:  
Chamber_Pressure = 68 MPa  
Chamber_Shape = Cylindrical
```

Chamber_Inner_Diameter	= 0.270 m
Chamber_Cylindrical_Length	= 0.500 m
Nozzle_Convergent_Section_Angle	= 45 degrees
Throat_Diameter	= 0.050 m
Wall_Curvature_Radius_at_Throat	= 0.050 m
Injector_Face	= Flat
Avg_Chamber_Gas_Temperature	= 2800 K
Avg_Chamber_Gas_Molecular_Weight	= 20 kg/kg-mol
Specific_Heat_Ratio (γ)	= 1.20

-- ASSUMPTION:
-- Gas composition and temperature are uniform throughout the cylindrical chamber section.

-- TASK 1:
-- Determine approximate resonance frequencies for:
-- - First longitudinal mode
-- - First radial mode
-- - First tangential mode

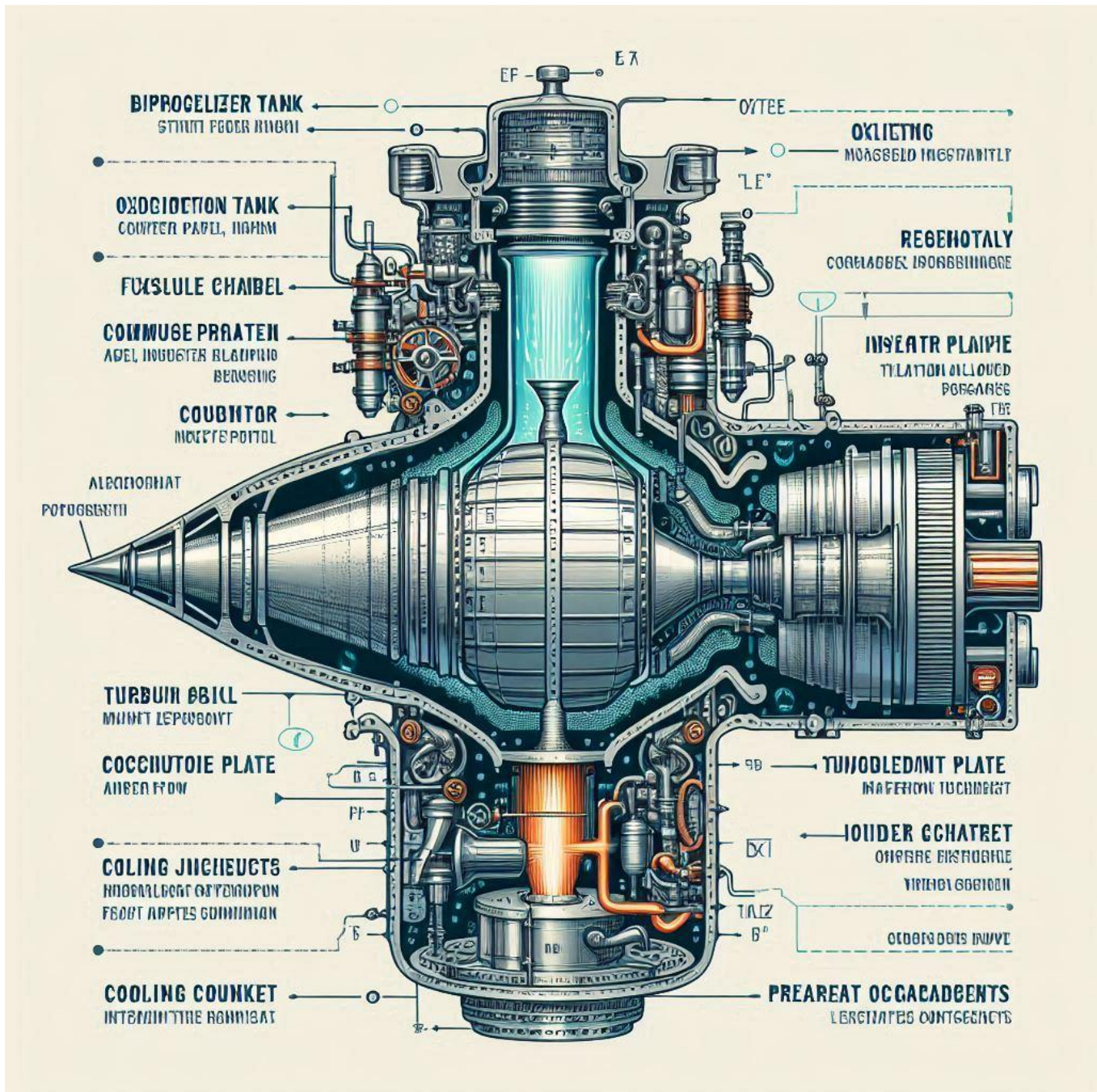
-- TASK 2:
-- Discuss how the three resonance frequencies change with:
-- - Combustion temperature ↑
-- - Chamber pressure ↑
-- - Chamber length ↑
-- - Chamber diameter ↑
-- - Throat diameter ↑

-- TASK 3:
-- Explain why heat transfer increases during combustion instabilities.

-- TASK 4:
-- List steps to validate the stability of a new pressure-fed medium-sized liquid bipropellant rocket engine.
-- Include all assumptions.

-- TASK 5:
-- Estimate the resonant frequency for a set of nine cavities (similar to Fig. 9-7):

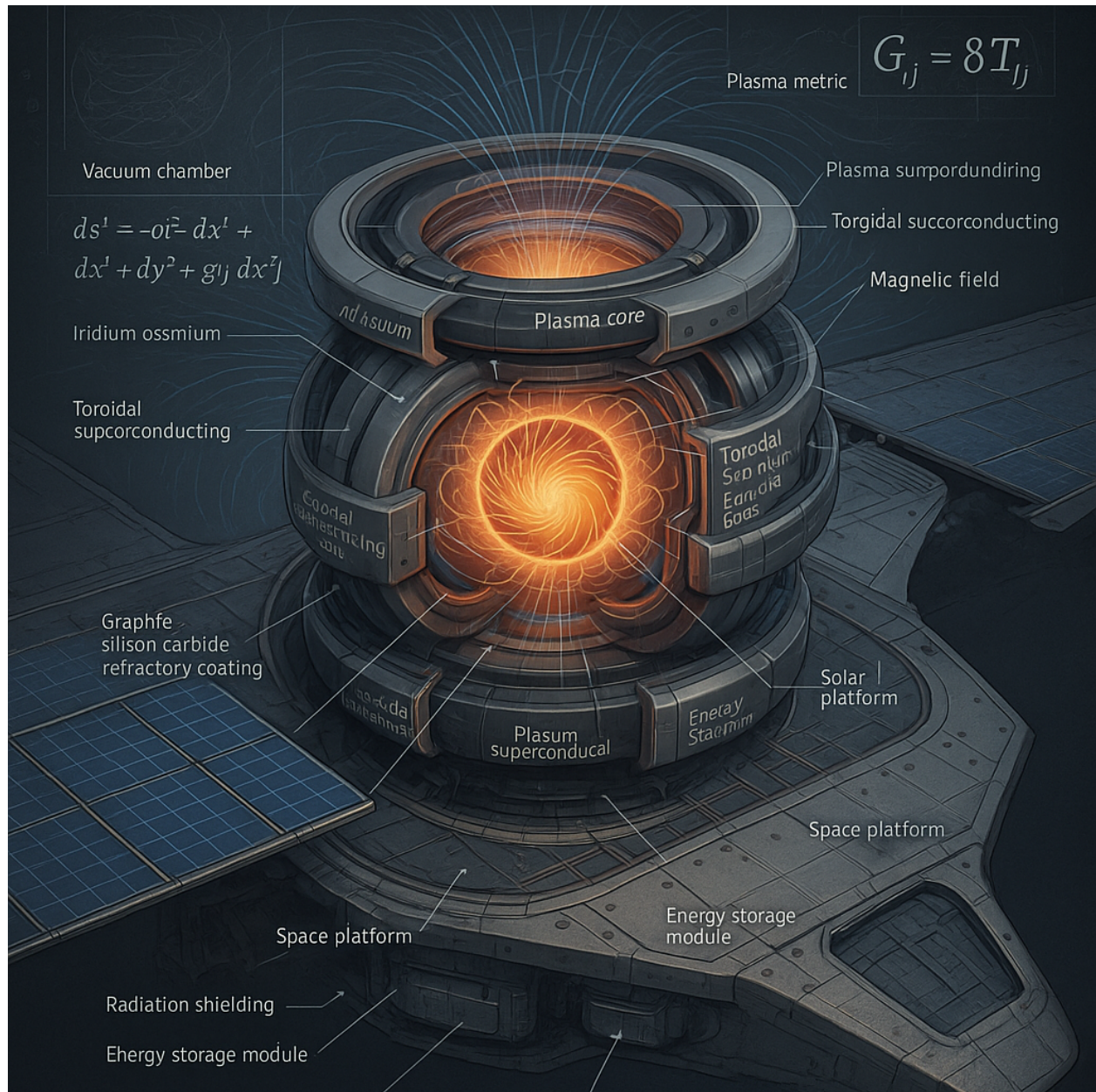
Chamber_Diameter	= 0.20 m
Slot_Width	= 1.0 mm
Cavity_Width	= 20.0 mm
Cavity_Height	= 20.0 mm
Wall_Thickness	= 10.0 mm
Cavity_Length (L)	= 4.0 mm
ΔL	= 2.0 mm
Speed_of_Sound (a)	= 1050 m/s



Inertial upper-stage (IUS) Orbus rocket motor with an extendible exit cone (EEC).

These are motorways for propelling upper launch vehicle stages or spacecraft. The grain was simple (internal tube perforation). With the EEC and a thrust vector control, the motor had a propellant mass fraction of 0.916. When launched, and while the two lower vehicle stages were operating, the two conical movable nozzle segments were stowed around the smaller inner nozzle segment. Each of the movable segments was then deployed in space and moved into

its operating position by three rotary actuators. The nozzle area ratio increased from 49.3 to 181; overall this improved the specific impulse by about 14 sec. This motor (without the EEC)



Nozzles

About 80 years ago nozzles were manufactured from a single piece of molded polycrystalline graphite and some were supported by metal housing structures.

They eroded easily, but were low in cost. We still use them today for short duration, low chamber pressure, low altitude flight applications with low thrust, such as in certain tactical missiles. For more

severe conditions a throat insert or ITE is placed into the graphite piece; this insert is a denser, better grade of graphite; later pyrolytic graphite washers and fiber-reinforced carbon materials came into use.

Figure 15–7 shows a set of non-isotropic pyrolytic graphite washers in the throat insert of small nozzles (they are not used now). For a period of time tungsten inserts were used; they had very good erosion resistance, but were heavy and their melting point was eventually exceeded as higher motor pressures and hotter propellants came into use. The introduction of high-strength carbon fibers in a carbon matrix has been a major advance in high-temperature materials. For small and medium-sized nozzles, ITE pieces have been made of carbon–carbon, the present abbreviation for carbon fibers in a carbon matrix. The orientation of the fibers can be two-directional (2D) or three-directional (3D), as described below. Some properties of these materials are listed in Tables 15–4 and 15–5. For large nozzles the then existing technology did not allow the fabrication of large 3D carbon–carbon ITE pieces, so layups of carbon fiber (or silicon fiber) cloths in a phenolic matrix were used. An example of a self-supporting ablative exit cone is the Naxeco-phenolic structure used in the first stage of the Vega launch vehicle.

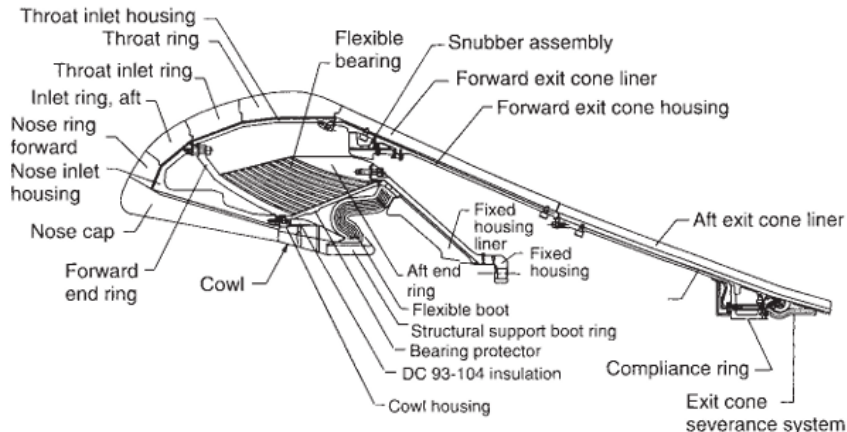


FIGURE 15–9. Section through movable nozzle shown in Fig. 15–8 with component identification. Courtesy of Orbital ATK

Typical Motor Nozzle Materials and Their Functions

- **Structural Support:**
 - Aluminum: used for housings, limited to ~515 °C (959 °F).
 - High-strength steels & special alloys: for 625–1200 °C (1157–2192 °F). Provide rigidity & pressure containment under heat.

- **Extreme Heat Zones (Throat, Inlet):**
 - Carbon–carbon composites (3D/4D woven carbon fibers):
 - Withstand up to 3300 °C (5972 °F).
 - High cost limits broader use.
 - Exceptional for thermal resistance.

- Insulation (Behind flame barriers):
 - Carbon/Kevlar fiber cloth w/ phenolic or plastic resin.
 - Molded graphite: cheap, for low-pressure chambers.
 - Tungsten & molybdenum: erosion resistant, but heavy & costly.

- Flame Barriers:
 - Ablative plastics (silica/Kevlar + phenolic resins):
 - Filament-wound or bonded.
 - Strong adhesion, low thermal conductivity.

- Exit Cone Materials:
 - Ablative plastics: less filler → more erosion-resistant.
 - Carbon/silica fibers + phenolic resin: woven/glued layups.
 - Carbon-carbon: 3D-layered for high-thermal exposure.
 - Self-supporting ablative plastics or hybrid supports used for short-burn designs.

- Refractory Metals for high-performance missions:
 - Niobium alloy (Cb-103), Tantalum (Ta), Molybdenum (Mo):
 - Strong, heavy, require oxidation protection.

- Radiation-cooled designs may use carbon-carbon for strength.

Carbon-Carbon Composites

- Made of oriented carbon fibers in carbon matrix.
 - Woven, needled, or laid-up configurations.
- Fiber orientations:
 - 2D: two directions.
 - 3D: orthogonal.
 - 4D: tetrahedral or hexagonal patterns.
 - Tetrahedral: equal in four cube-diagonals.
 - Hexagonal: 3 directions at 60° in a plane + axial.

- Highly densified types: superior in heat transfer zones (throat).
 - Can resist steep temp gradients due to multidirectional reinforcement.

- Matrix formed via:
 - Chemical Vapor Deposition (CVD)
 - Liquid impregnation + pyrolysis.

- Notable materials:
 - Naxeco Sepcarb & 3D-reinforced phenolic (by Herakles - Vega flights).
 - Carbon-SiC & refractory metal nozzles in modern production.

Ablative Materials

- High-temp fiber reinforcements:
 - Silica glass, Kevlar, carbon fibers.

- Impregnated with phenolic/epoxy resins.
- Fiber forms: strands, woven cloth, ribbons (machine wound).

IGNITER HARDWARE

→ Role:

- Initiates propellant ignition.
- Mass <1% of total propellant.
- Must be minimal in mass but reliable.

→ Igniter Locations:

- Forward mounting → gas over grain helps ignition.

→ Pyrotechnic Igniters:

- Use small solid propellant pellets.
- High surface area, short burn time.
- Common types: pellet basket, powder can, jellyroll, etc.

→ Ignition Sequence:

1. Electrical signal → squib/primer charge.
 2. Squib ignites booster.
 3. Booster ignites main charge.
- Example: 24% Boron + 71% KCLO₄ + 5% binder.

→ Pyrogen Igniters:

- Mini rocket motors, not for thrust.
- Use motor-like grain + nozzles.
- Heat transfer via convection (unlike pyrotechnic → radiation).
- Often external; jet injected through main nozzle.

Electric Initiators

- Names: squibs, glow plugs, primers, headers.
- Always first in ignition train; also act as safety.

→ Common Types:

- (a) Diaphragm style: sends shock wave to acceptor charge.
- (b) Glow plug: high-resistance bridgewires in charge.
- (c) Exploding wire: 0.02-0.10 mm platinum/gold wire vaporized by high-voltage pulse.

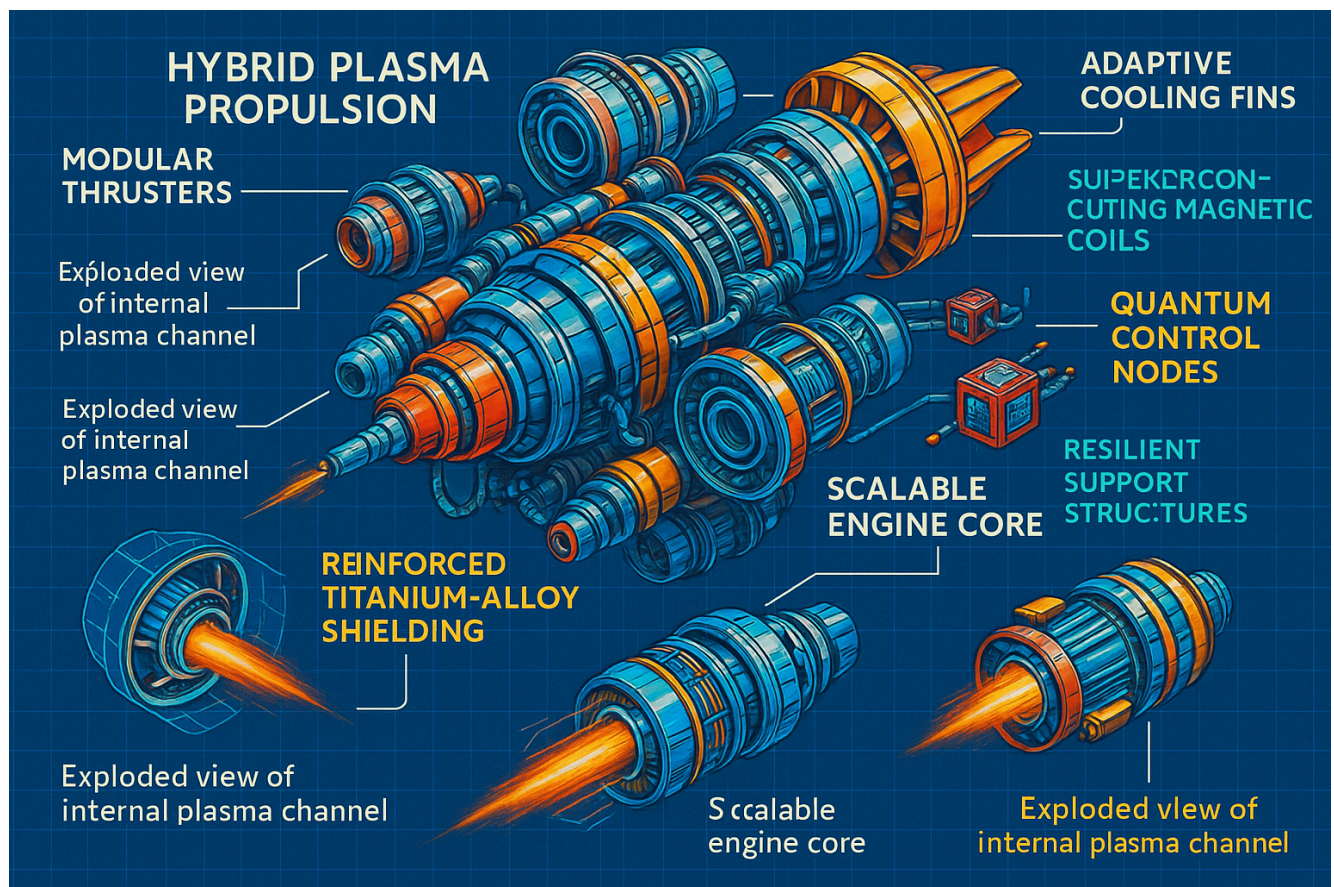
Igniter Analysis & Design

- Models of heat transfer, flame spread, chamber fill are incomplete.
- Design relies heavily on experimental data.
- Empirical formula for igniter charge mass:
 $m = 0.12 \times (VF)^{0.7}$

where:

$$m = \text{igniter charge (grams)}$$
$$VF = \text{motor free volume (in}^3\text{)}$$

- Larger igniter → faster ignition.
- Ignition sequence timing illustrated in Fig. 14-3 (not shown here).



Vehicles:

- 1) Many early hybrid rocket motor developments focused on target missiles and low-cost small tactical missile applications. Other development efforts concentrated on high-energy upper-stage motors. In one program, a hybrid motor was developed for high-performance upper-stage applications, with design requirements including a nominal thrust of 22,240 Newtons and an 8:1 throttling range. This motor used oxygen difluoride as the oxidizer combined with a lithium hydride/polybutadiene fuel grain, both of which are highly toxic materials. More recently, development has shifted towards prototypes intended for space launch applications.

2) A more practical, though lower-energy, upper-stage hybrid propellant system uses high-test hydrogen peroxide (90 to 95% concentration) as the oxidizer paired with hydroxyl-terminated polybutadiene (HTPB) as the fuel. Hydrogen peroxide is considered storable for time periods typical of upper-stage missions, which usually last several months, and it is relatively inexpensive. In solid rocket motors, HTPB serves as a binder that consolidates aluminum fuel with an ammonium perchlorate oxidizer matrix. However, in hybrid motors, HTPB is the entire fuel component. It is low cost, easy to process, and does not self-deflagrate under known conditions.

A common propellant combination for large hybrid booster applications is liquid oxygen (LOX) as the oxidizer with HTPB as the fuel. Liquid oxygen is a widely used cryogenic oxidizer in the space launch industry because it is relatively safe, provides high performance, and is low in cost. This hybrid propellant pairing produces a non-toxic, reasonably smoke-free exhaust. It is favored for future booster applications since its chemical and performance characteristics are comparable to those of LOX-kerosene bipropellant systems.

3) While metallized solid fuels can increase performance, metals such as beryllium are very toxic, boron is difficult to ignite, lithium has a low heat of combustion, and aluminum oxides tend to increase the molecular mass of combustion products, often reducing the temperature gain. Research is ongoing on hydrides and slurries containing these metals to try to offset their disadvantages, but this work is still in early stages. On the other hand, hydrogen peroxide (H_2O_2) and hydroxyl ammonium nitrate (HAN) have proven to have desirable thermochemical properties, produce non-toxic exhausts, and offer attractive density-specific impulses. Their regression rates and combustion efficiencies are comparable to those of LOX, but they offer advantages in storage and are considered environmentally friendly.

In some applications where a smoky or highly radiative exhaust is acceptable, powdered aluminum may be added to the fuel. This increases the combustion temperature, reduces the stoichiometric mixture ratio, and increases both the fuel density and the overall density-specific impulse. However, while the density-specific impulse increases, adding aluminum may actually reduce the actual specific impulse. Theoretical vacuum-specific impulse values calculated at 1000 psi chamber pressure and a 10:1 nozzle expansion ratio illustrate performance differences among various cryogenic and storable oxidizers.

Interior Hybrid Motor Ballistics

In classical hybrid motors, the fuel grain contains no oxidizer, so combustion occurs only in the gaseous phase. This means that fuel surface regression rates differ significantly from those in solid rocket motors. Since the solid fuel must vaporize before burning, the fuel surface regression is closely related to the interaction of fluid dynamics within the combustion port and heat transfer to the fuel surface. The main combustion region is confined to a narrow flame zone located within the boundary layer that forms and grows over the fuel grain surface. Heat transfer to the fuel grain occurs by convection and radiation. Because hybrid motor behavior is largely empirical, the characteristics of any specific motor strongly depend on the propellant combination, the scale, and the combustion chamber design. Even though the payload of a multistage rocket represents a small fraction of the total initial mass, it is roughly proportional to the takeoff mass. For example, a 50 kg payload might require a 6000 kg multistage rocket, so scaling up to a 500 kg payload would need a roughly 60,000 kg rocket with the same number of stages and similar configuration, assuming the same payload fraction and propellant choice. When the upper

stage begins operation immediately after the lower stage's thrust ends, the total ideal velocity increment of a multistage vehicle arranged in series (tandem) is the sum of the velocity increments provided by each stage.

Flight Vehicles

Launch vehicles assemble individual stages in various geometric configurations. For n stages arranged in series, the final velocity increment is the sum of the velocity increments from each stage. In vertical atmospheric flight, these increments are determined by the rocket equation considering gravity and atmospheric drag. For a simplified case of vacuum flight without gravity, the velocity increment can be expressed as the sum of terms involving the natural logarithm of the mass ratios of each stage.

In two- or three-stage vehicles, the overall vehicle mass ratio (initial mass at takeoff to final mass after the last stage) can exceed 100. Different regions in performance charts correspond to single-stage vehicles (mass ratio up to about 95) and multistage vehicles (mass ratio beyond 180).

Stage Separation

When a lower stage ends thrust, it takes a finite time (1 to 3 seconds for large engines, less for small ones) for thrust to drop to zero. Additional delays of 4 to 10 seconds may be needed for physical separation between stages before the upper stage engine can start. This delay prevents damage from hot exhaust plumes to the upper stage. Engine start-up is not instantaneous and can take several seconds in large rocket systems. During these delays, gravity slows the vehicle, reducing its velocity by 7 to 160 meters per second. "Hot staging" is a technique used to reduce velocity losses and shorten the time between stages.

Two-Stage Vehicle Example

Consider a two-stage vehicle launched from a high-orbit satellite in a gravity-free vacuum trajectory. Using the following notation:

- $m_0m_0m_0$: initial mass of the vehicle or stage at launch
- mpm_pmp : propellant mass of the stage
- mim_imi : initial mass of a stage (including propellant and structure)
- mfm_fmf : final mass after burn (empty stage plus residual propellant, structure, control, guidance, payload)
- $mplm_pl\{pl\}mpl$: payload mass, including scientific instruments, guidance and control, communication equipment, power supply, etc.

For both stages:

- Flight velocity increment: 4700 m/s
- Specific impulse: 310 seconds
- Initial total launch mass: 4500 kg
- Propellant mass fraction per stage: 0.88
- Same propellant used in both stages
- No stage separation delay assumed

Plasma Structures Inside Hybrid Propulsion Systems – Design Example

For designing a large hybrid booster, preliminary design parameters can be determined as follows:

- Fuel: HTPB
- Oxidizer: Liquid oxygen (LOX)
- Required booster initial thrust (vacuum): 3.1 million pounds-force
- Burn time: 120 seconds
- Fuel grain outside diameter: 150 inches
- Initial chamber pressure: 700 psi absolute
- Initial mixture ratio (oxidizer to fuel mass): 2.0
- Initial nozzle area ratio: 7.72
- Ambient pressure: 14.696 psi (sea level)

STAGES:

High initial thrust or high initial acceleration for the missile to quickly reach a high-initial-powered flight velocity. See Fig. 12–19.

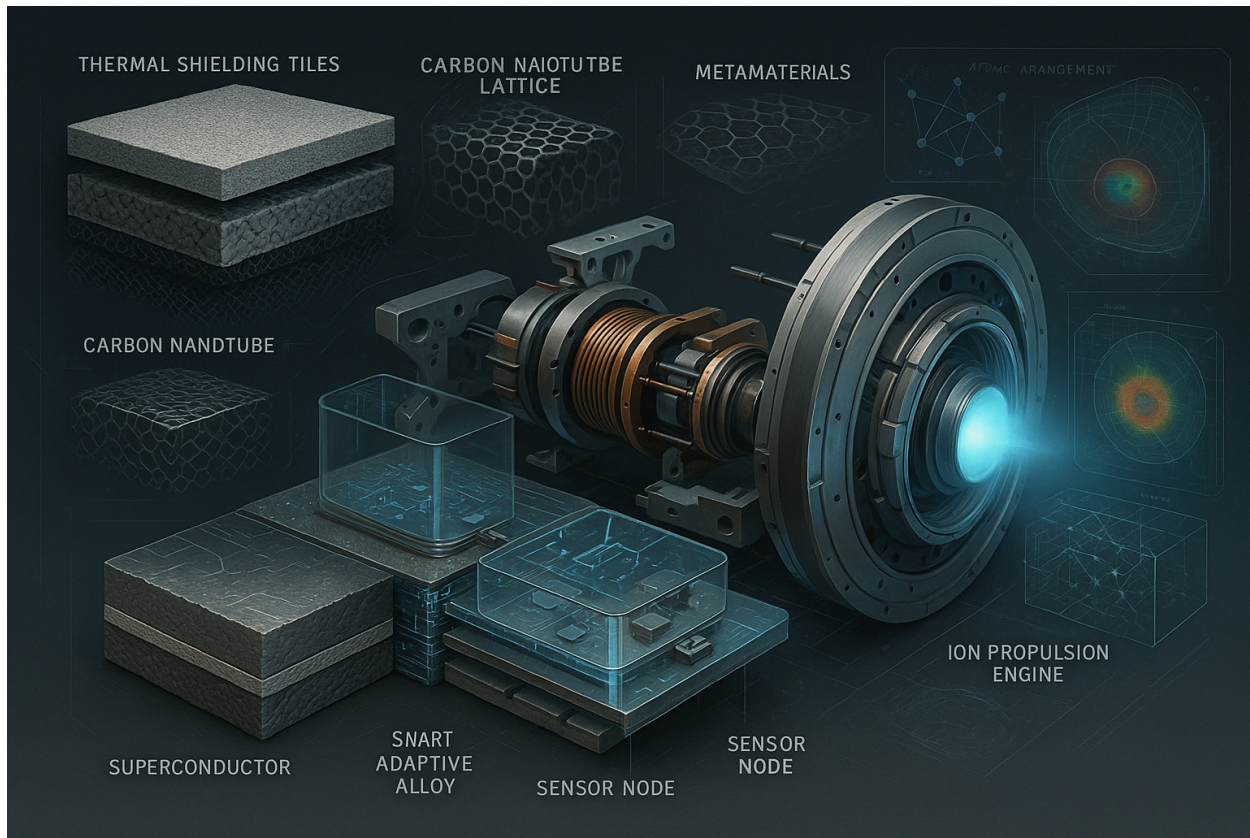
Application of a subsequent lower thrust to counteract drag and gravity losses and thus maintain the high flight velocity. This can be done with a single rocket propulsion system that gives a short high initial thrust followed by a smaller (10 to 25%) sustaining thrust of longer duration.

For the higher supersonic flight speeds, a two-stage missile can be more effective. Here, the first stage is dropped off after its propellant has been consumed, thus reducing the inert mass of the next stage and improving its mass ratio and thus its flight velocity increase.

If the target is highly maneuverable and if the closing velocity between missile and target is large, it may be necessary not only to provide an axial thrust but also to apply large side forces or side accelerations to a defensive missile. This can be accomplished either by aerodynamic forces (lifting surfaces or flying at an angle of attack) or by multiple-nozzle propulsion systems with variable or pulsing thrusts; the rocket engine then would have an axial thruster and one or more side thrusters. The side thrusters have to be so located that all the thrust forces are essentially directed through the center of gravity of the vehicle in order to minimize turning moments. Thrusters that provide the side accelerations have also been called divert thrusters, since they divert the vehicle in a direction normal to the axis of the vehicle.

Drag losses can be reduced when the missile has a large L/D ratio (or a small cross-sectional area) and when the propellant density is high, allowing a smaller missile volume. Drag forces are highest when missiles travel at low altitudes and high speeds. Long and thin propulsion system configurations and high-density propellants help to reduce drag.

The combustion of hydrogen with oxygen is used below as an example. It may yield six possible products: water, hydrogen, oxygen, hydroxyl, atomic oxygen, and atomic hydrogen. Here, all reactants and products are gaseous.



Theoretically, there could be two additional products: ozone O₃ and hydrogen peroxide H₂O₂; however, these are unstable compounds that do not exist for long at high temperatures and can be ignored. In chemical notation the mass balance may be stated as a H₂ + b O₂ → n H₂O + nH₂ H₂ + nO₂ O₂ + nO O + nH H + nOH OH

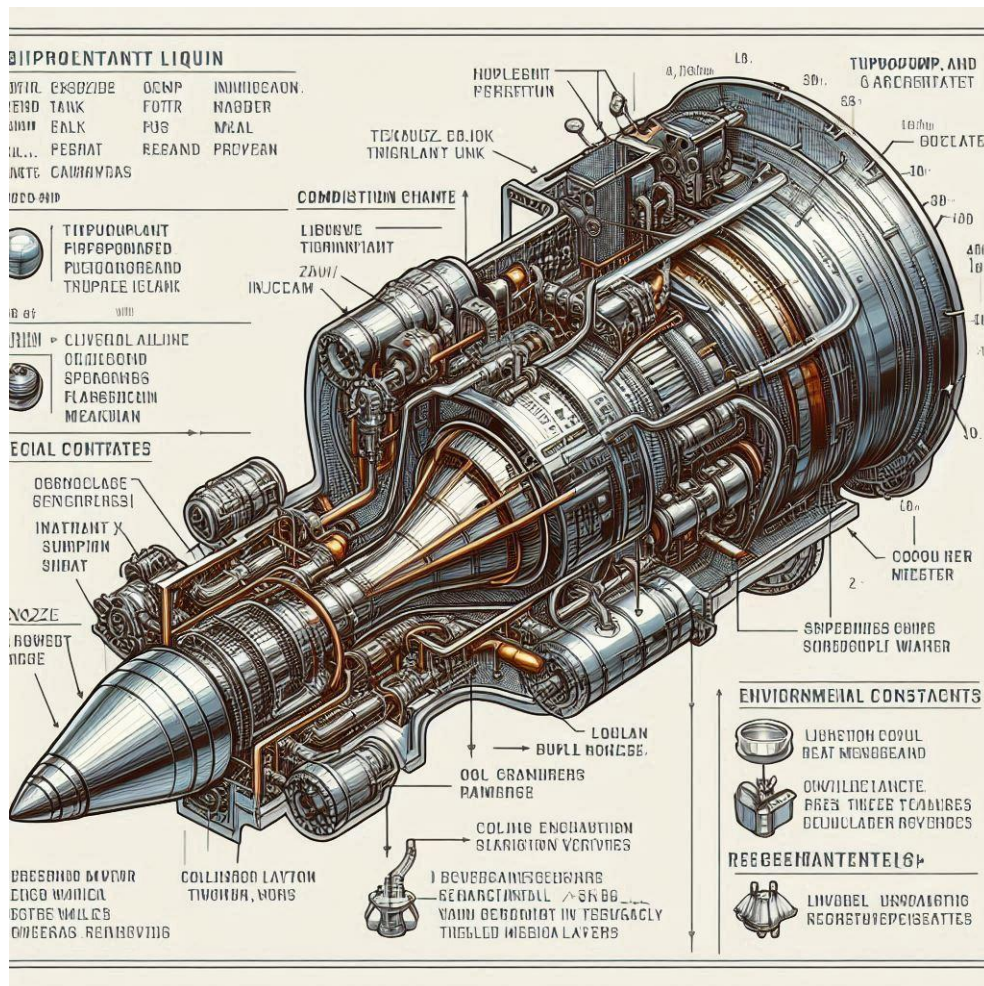
The left side shows the condition before the reaction and the right side the condition after. Since H₂ and O₂ are found on both sides, it means that not all of these species are consumed and a portion, namely, nH₂ and nO₂, will remain unreacted. At any particular temperature and pressure, the molar concentrations on the right side will remain fixed when chemical equilibrium prevails. Here, a, b, nH₂O, nH₂, nO₂, nO, nH.

PYTHON

```

kg-mol of species j, and m and r are indices as defined above. The
average molecular
mass for the products, using Eqs. 5-5 and 5-19, becomes
M =
2 nH2 + 32 nO2 + 18 nH2O + 16 nO + nH + 17 nOH
-----
nH2 + nO2 + nH2O + nO + nH + nOH
(5-22)

```



PYTHON

The computational approach used in Ref. 5-13 is the one commonly used today for thermochemical analyses. It relies on the minimization of the Gibbs free energy and on the mass balance and energy balance equations. As was indicated in Eqs. 5-12 and 5-13, the change in the Gibbs free energy function is zero at equilibrium; here, the chemical potential of the gaseous propellants has to equal that of the gaseous reaction products, which is Eq. 5-12:

$$\Delta G = \sum (n_i \Delta G_i)_{\text{products}} - \sum (n_i \Delta G_i)_{\text{reactants}} = 0$$

Theory:

The energy release efficiency, sometimes called the combustion efficiency, can be defined here as the ratio of the actual change in enthalpy per unit propellant mixture to the calculated change in enthalpy necessary to transform the reactants from the initial conditions to the products at the chamber temperature and pressure. The actual enthalpy change is evaluated when the initial propellant conditions and the actual compositions and the temperatures of the combustion gases are measured. Measurements of combustion temperature and gas composition are difficult to perform accurately, and combustion efficiency is therefore only experimentally evaluated in rare instances (such as in some R & D programs). Combustion efficiencies in liquid propellant rocket thrust chambers also depend on the method of injection and mixing and increases with increasing combustion temperature. In solid propellants the combustion efficiency becomes a function of grain design, propellant composition, and degree of uniform mixing among the several solid constituents. In well-designed rocket propulsion systems, actual measurements yield energy release efficiencies from 94 to 99%.

Implementing CEA calculations using Cantera:[CEA](#) (Chemical Equilibrium with Applications) is a classic NASA software tool developed for analyzing combustion and rocket propulsion problems. It was written in Fortran, but is available to run via a [web interface](#).

Given rocket propellants, CEA can not only determine the combustion chamber equilibrium composition and temperature, but also calculate important rocket performance parameters.

Although CEA is extremely useful, it cannot (easily) be used within Python. Plus, we might want to [Cantera](#) is a modern software library for solving problems in chemical kinetics, thermodynamics, and transport, that offers a Python interface. Cantera natively supports phase and chemical equilibrium solvers. In particular, it can simulate finite-rate chemical reactions.

```
# this line makes figures interactive in Jupyter notebooks
%matplotlib inline
from matplotlib import pyplot as plt

import numpy as np
import cantera as ct

from pint import UnitRegistry
ureg = UnitRegistry()
Q_ = ureg.Quantity

# for convenience:
def to_si(quant):
    '''Converts a Pint Quantity to magnitude at base SI units.
    '''
    return quant.to_base_units().magnitude
```

Given a fixed temperature and pressure, determine the equilibrium composition of chemical species. This problem is relevant to an isothermal process, or where temperature is a design variable, such as in nuclear thermal or electrothermal rockets.

For example, say we have gaseous hydrazine (N_2H_4) as a propellant, with a chamber temperature of 5000 K and pressure of 50 psia. For this system, determine the equilibrium composition.

In [CEA](#), this is a **tp** problem, or fixed temperature and pressure problem. We should expect that, at such high temperatures, the equilibrium state will have mostly one- and two-atom molecules, based on the elements present: N_2 , H_2 , H , N , and HN .

ANALYSIS OF NOZZLE EXPANSION PROCESSES

There are several methods for analyzing the nozzle flow, depending on the chemical equilibrium assumptions made, nozzle expansion particulates, and/or energy losses. Several are outlined in the python Scripts.

The viscous boundary layers adjacent to nozzle walls have velocities substantially lower than those of the inviscid free stream. This viscous drag near the walls actually causes a conversion of kinetic energy into thermal energy, and thus some parts of the boundary layer can be hotter than the local free-stream static temperature. A diagram of a two-dimensional boundary layer is shown in Figure 3–15. With turbulent flows, this boundary layer can be relatively thick in small nozzles. Boundary layers also depend on the axial pressure gradient in the nozzle, nozzle geometry (particularly at the throat region), surface roughness, and/or the heat losses to the nozzle walls. The layers immediately adjacent to the nozzle walls always remain laminar and subsonic. Presently, boundary layer analyses with unsteady flow are only approximations, but are expected to improve as our understanding of relevant phenomena grows and as computational fluid dynamics (CFD) techniques improve. The net effect of such viscous layers appears as nonuniform velocity and temperature profiles, irreversible heating (and therefore increases in entropy), and minor reductions (usually less than 5%) of the kinetic exhaust energy for well-designed systems.

Once the gases reach a supersonic nozzle, they experience an adiabatic, reversible expansion process which is accompanied by substantial drops in temperature and pressure, reflecting the conversion of thermal energy into kinetic energy. Several increasingly more complicated methods have been used for analyzing nozzle processes.

For the simplest case, frozen (composition) equilibrium and one-dimensional flow, the state of the gas throughout expansion in the nozzle is fixed by the entropy of the system, which is considered to be invariant as the pressure is reduced. All assumptions listed in Chapter 3 for ideal rockets would be valid here. Again, effects of friction, divergence angle, heat losses, shock waves, and nonequilibrium are neglected in the simplest cases but are considered for the more sophisticated solutions. Any condensed (liquid or solid) phases present are similarly assumed to have zero volume and to be in kinetic as well as thermal equilibrium with the gas flow. This implies that particles and/or droplets are very small in size, move at the same velocity as the gas stream, and have the same temperature as the gas everywhere in the nozzle.

5.3. ANALYSIS OF NOZZLE EXPANSION PROCESSES

Chemical composition during nozzle expansion may be treated analytically in the following ways:

1. When the expansion is sufficiently rapid, composition may be assumed as invariant throughout the nozzle, that is, there are no chemical reactions or phase changes and the reaction products composition at the nozzle exit are identical to those of the chamber. Such composition results are known as frozen equilibrium rocket performance. This approach is the simplest, but tends to underestimate the system's performance typically by 1 to 4%.
2. Instantaneous chemical equilibrium among all molecular species may be significant in some cases under the continuously variable pressure and temperature conditions of the nozzle expansion process. Here, product compositions do shift because the chemical reactions and phase change equilibria taking place between gaseous and condensed phases in all exhaust gas species are fast compared to their nozzle transit time. The composition results so calculated are called shifting equilibrium performance. Here, gas composition mass fractions are different at the chamber and nozzle exits. This method usually overstates real performance values, such as c^* or I_s , typically by 1 to 4%. Such analysis is more complex and many more equations are needed.
3. Even though the chemical reactions may occur rapidly, they do require some finite time. Reaction rates for specific reactions are often estimated; these rates are a function of temperature, the magnitude of deviation from the equilibrium molar composition, and the nature of the chemicals or reactions involved. Values of T , c^* , or I_s in most types of actual flow analyses usually fall between those of frozen and instantaneously shifting equilibria. This approach is seldom used because of the lack of good data on reaction rates with multiple simultaneous chemical reactions.

The simplest nozzle flow analysis is also one dimensional, which means that all velocities and temperatures or pressures are equal at any normal cross section of an axisymmetric nozzle. This is often satisfactory for preliminary estimates. In two-dimensional analyses, the resulting velocity, temperature, density, and/or Mach number do not have a flat profile varying somewhat over the cross sections. For nozzle shapes that are not bodies of revolution (e.g., rectangular, scarfed, or elliptic), three-dimensional analyses need to be performed.

When solid particles or liquid droplets are present in the nozzle flow and when the particles are larger than about $0.1 \mu\text{m}$ average diameter, there will be both a thermal lag and a velocity lag. Solid particles or liquid droplets cannot expand as a gas; their temperature decrease depends on how they lose energy by convection and/or radiation, and their velocity depends on the drag forces exerted on the particle.

Larger-diameter droplets or particles are not accelerated as rapidly as smaller ones and their flow velocities are lower than those of the accelerating gases. Also, these particles remain hotter than the gas and provide heat to it.

CEA_Python:

```
# extract all species in the NASA database
full_species = {S.name: S for S in
ct.Species.list_from_file('nasa_gas.yaml')}
```

```

# extract only the relevant species
species = [full_species[S] for S in (
    'N2H4', 'N2', 'H2', 'H', 'N', 'NH'
)]
gas = ct.Solution(thermo='ideal-gas', species=species)

temperature = Q_(5000, 'K')
pressure = Q_(50, 'psi')

gas.TPX = to_si(temperature), to_si(pressure), 'N2H4:1.0'
gas.equilibrate('TP')
gas()

```

The current system of N2H4,

Ne=2 and thus there are six unknowns. Since this is a linear system of equations, we can solve it using linear algebra, via NumPy's `linalg.solve` function. Let's set up a function to solve this system:

PYTHON-Hardware

```

def get_thermo_derivatives(gas):
    '''Gets thermo derivatives based on shifting equilibrium.
    '''

    # unknowns for system with no condensed species:
    # dpi_i_dlogT_P (# elements)
    # dlogn_dlogT_P
    # dpi_i_dlogP_T (# elements)
    # dlogn_dlogP_T
    # total unknowns: 2*n_elements + 2

    num_var = 2 * gas.n_elements + 2

    coeff_matrix = np.zeros((num_var, num_var))
    right_hand_side = np.zeros(num_var)

    tot_moles = 1.0 / gas.mean_molecular_weight
    moles = gas.X * tot_moles

    condensed = False

    # indices
    idx_dpi_dlogT_P = 0
    idx_dlogn_dlogT_P = idx_dpi_dlogT_P + gas.n_elements
    idx_dpi_dlogP_T = idx_dlogn_dlogT_P + 1
    idx_dlogn_dlogP_T = idx_dpi_dlogP_T + gas.n_elements

```

```

# construct matrix of elemental stoichiometric coefficients
stoich_coeffs = np.zeros((gas.n_elements, gas.n_species))
for i, elem in enumerate(gas.element_names):
    for j, sp in enumerate(gas.species_names):
        stoich_coeffs[i,j] = gas.n_atoms(sp, elem)

# equations for derivatives with respect to temperature
# first n_elements equations
for k in range(gas.n_elements):
    for i in range(gas.n_elements):
        coeff_matrix[k,i] = np.sum(stoich_coeffs[k,:] * 
stoich_coeffs[i,:]* moles)
        coeff_matrix[k, gas.n_elements] = np.sum(stoich_coeffs[k,:] * 
moles)
        right_hand_side[k] = -np.sum(stoich_coeffs[k,:] * moles * 
gas.standard_enthalpies_RT)

    # skip equation relevant to condensed species

    for i in range(gas.n_elements):
        coeff_matrix[gas.n_elements, i] = np.sum(stoich_coeffs[i, :] * 
moles)
        right_hand_side[gas.n_elements] = -np.sum(moles * 
gas.standard_enthalpies_RT)

# equations for derivatives with respect to pressure

for k in range(gas.n_elements):
    for i in range(gas.n_elements):
        coeff_matrix[gas.n_elements+1+k,gas.n_elements+1+i] =
np.sum(stoich_coeffs[k,:]* stoich_coeffs[i,:]* moles)
        coeff_matrix[gas.n_elements+1+k, 2*gas.n_elements+1] =
np.sum(stoich_coeffs[k,:]* moles)
        right_hand_side[gas.n_elements+1+k] = np.sum(stoich_coeffs[k,:] * 
moles)

    for i in range(gas.n_elements):
        coeff_matrix[2*gas.n_elements+1, gas.n_elements+1+i] =
np.sum(stoich_coeffs[i, :] * moles)
        right_hand_side[2*gas.n_elements+1] = np.sum(moles)

    derivs = np.linalg.solve(coeff_matrix, right_hand_side)

    dpi_dlogT_P = derivs[idx_dpi_dlogT_P : idx_dpi_dlogT_P + 
gas.n_elements]
    dlogn_dlogT_P = derivs[idx_dlogn_dlogT_P]
    dpi_dlogP_T = derivs[idx_dpi_dlogP_T]
    dlogn_dlogP_T = derivs[idx_dlogn_dlogP_T]

    # dpi_dlogP_T is not used

```

```
return dpi_dlogT_P, dlogn_dlogT_P, dlogn_dlogP_T
```

MOLS_SIMULATION_ALGORITHMS

n mols of liquid water, producing n + 2 mol of water vapor plus 1 mol of oxygen gas. Since the reaction goes to completion, no equilibrium constant is needed:

$$2 \text{ H}_2\text{O}_2(\text{l}) + n \text{ H}_2\text{O}(\text{l}) \rightarrow (n + 2) \text{ H}_2\text{O}(\text{g}) + \text{O}_2(\text{g})$$

The symbols (l) and (g) refer to the liquid state and the gaseous state, respectively. The heats of formation from the standard state $\Delta_f H_0$ and molar specific heats Cp are shown below (see Table 5-1 and other common sources such as the NIST Chemistry Web-Book, <http://webbook.nist.gov/chemistry/>). For these calculations the heat of mixing may be ignored.

Species	$\Delta_f H_0$ (kJ/kg-mol)	Cp (J/kg-mol-K)	\bar{m} (kg/kg-mol)
H ₂ O ₂ (l)	-187.69	34.015	
H ₂ O(l)	-285.83	18.015	
H ₂ O(g)	-241.83	0.03359	18.015
O ₂ (g)	0	0.02938	31.999

The energy balance, Eq. 5-9, for 2 mol of decomposing hydrogen peroxide becomes

$$\begin{aligned}\Delta_r H_0 &= [n \Delta_f H_0]_{\text{H}_2\text{O}} - [n \Delta_f H_0]_{\text{H}_2\text{O}_2} \\ &= 2 \times (-241.83) - 2 \times (-187.69) \\ &= -108.28 \text{ kJ}\end{aligned}$$

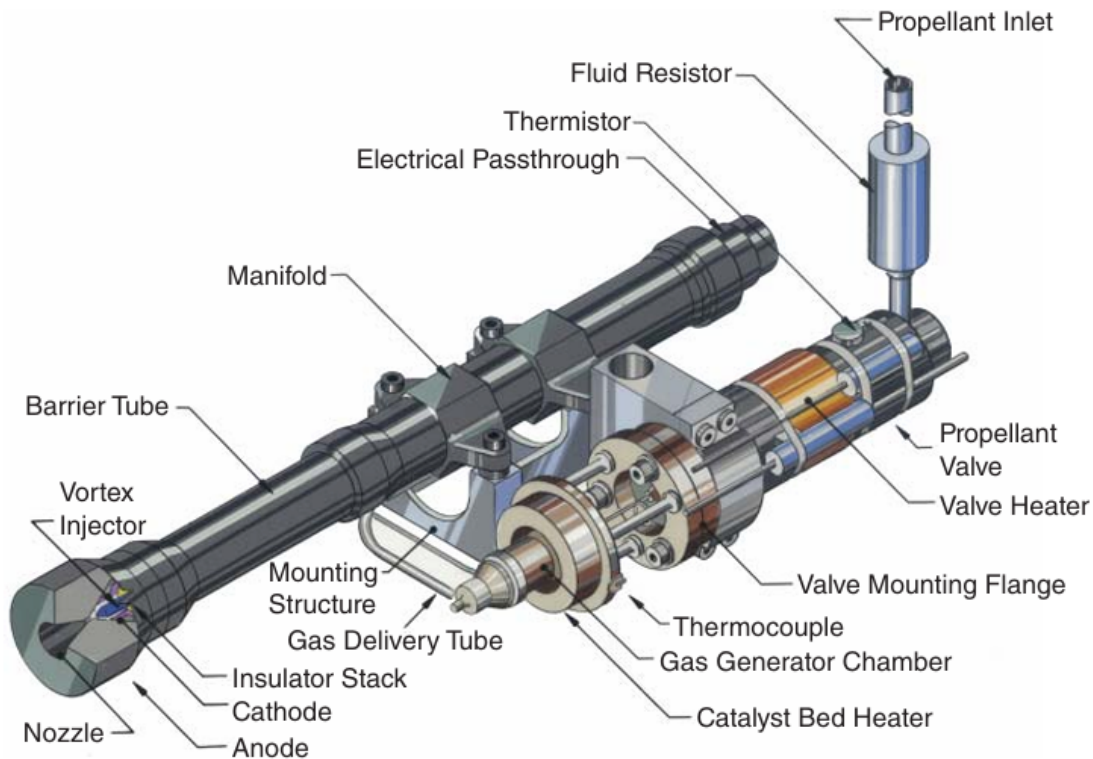


FIGURE 17–6. Perspective drawing of a 2-kW arcjet thruster. Its performance is initially augmented by the catalytic-decomposition of hydrazine into moderately hot gases, which are in turn fed through an electric arc and further heated. The arc is located at the centerline of the flow passage at the throat region of a converging-diverging nozzle. Courtesy of Aerojet Rocketdyne, Redmond Operations

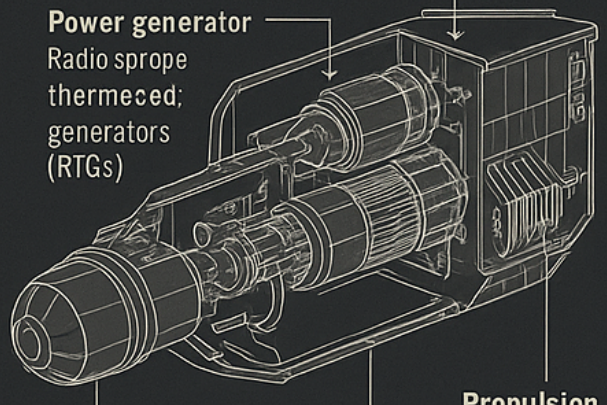
PROPUSSION

Main Engine

Liquid (ironLengening
RTGs: Plutonium 239
TWde: CB,NF

Power generator

Radioisotope
thermoelectric
generators
(RTGs)



Radioisotope thermoelectric generators (RTGs)

Propulsion

Thickness 2,5 cm
(in)

Scientific instruments

Solid-state camera
200 x 300 pixels
Wavelength, 365 nm
Plutonium, 238 b
Mass: 29 kg (65 lb)

Sclintetra. mapping spectrometer

256 x 256 pm
Mass 18 kg (1)

SCIENTIFIC INSTRUMENTS

Solid-state

Camera:



Solid-state
900 x 300 pixels

Near-infrared mapping spectrometer

255 x 250 pixel
Mass 18 kg (1)

Near-Infrared mapping spectro-

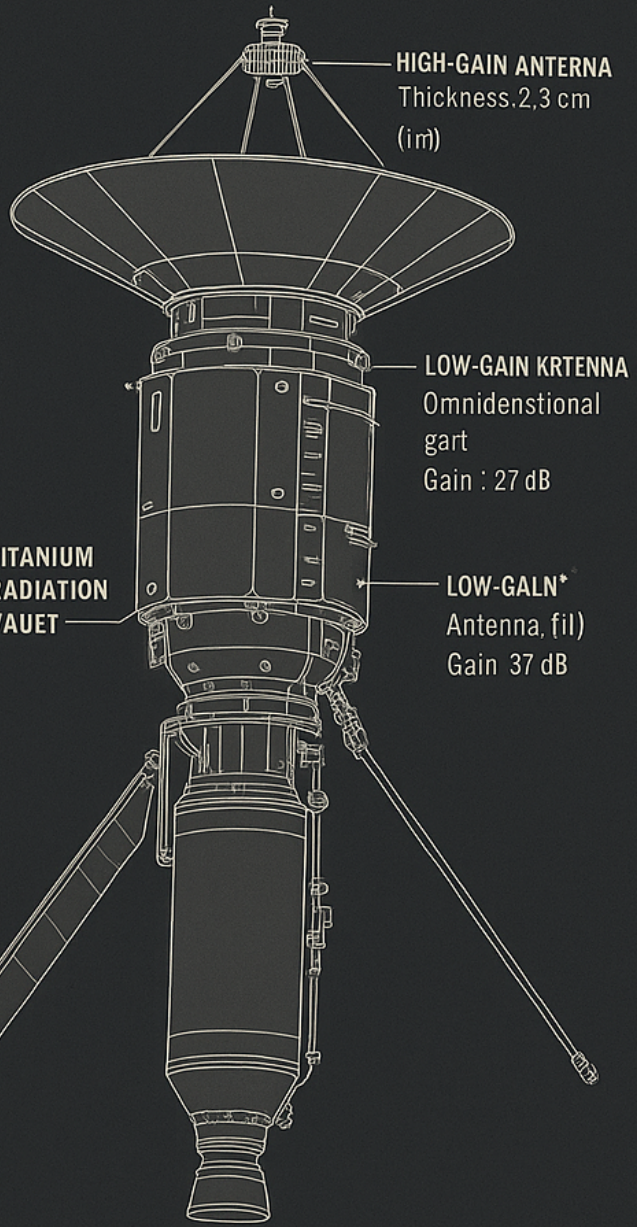
256 x 256 pm

Propulsion

2,5 cm (in)
Mass 18 kg (6)

HIGH-GAIN ANTENNA

Thickness 2,3 cm
(in)



LOW-GAIN OMNIDIRECTIONAL ANTENNA

Gain : 27 dB

LOW-GAIN ANTENNA

Antenna, fil)
Gain 37 dB



The reaction is exothermic but, as stated, some of this energy is used up in vaporizing the diluent liquid water, namely, $285.83 - 241.83 = 44.0 \text{ kJ/kg-mol}$ (at standard conditions). The net available heat release thus becomes $108.28 - 44.0 n \text{ (kJ)}$. In order to calculate the adiabatic temperature, we assume ideal-gas heating at constant pressure, Eq. 5–18 (values for the molar specific heats are from Table 5–1 and are taken as constant):

$$\int (n_{\text{H}_2\text{O}} C_p_{\text{H}_2\text{O}} + n_{\text{O}_2} C_p_{\text{O}_2}) dT = [(2 + n) C_p_{\text{H}_2\text{O}} + C_p_{\text{O}_2}] \Delta T = 108.28 - 44.0 n$$

```

def get_thermo_properties(gas, dpi_dlogT_P, dlogn_dlogT_P,
dlogn_dlogP_T):
    '''Calculates specific heats, volume derivatives, and specific heat
ratio.

    Based on shifting equilibrium for mixtures.
    '''

    tot_moles = 1.0 / gas.mean_molecular_weight
    moles = gas.X * tot_moles

    # construct matrix of elemental stoichiometric coefficients
    stoich_coeffs = np.zeros((gas.n_elements, gas.n_species))
    for i, elem in enumerate(gas.element_names):
        for j, sp in enumerate(gas.species_names):
            stoich_coeffs[i,j] = gas.n_atoms(sp, elem)

    spec_heat_p = ct.gas_constant * (
        np.sum([dpi_dlogT_P[i] *
            np.sum(stoich_coeffs[i,:] * moles * gas.standard_enthalpies_RT)
            for i in range(gas.n_elements)
        ]) +
        np.sum(moles * gas.standard_enthalpies_RT) * dlogn_dlogT_P +
        np.sum(moles * gas.standard_cp_R) +
        np.sum(moles * gas.standard_enthalpies_RT**2)
    )

    dlogV_dlogT_P = 1 + dlogn_dlogT_P
    dlogV_dlogP_T = -1 + dlogn_dlogP_T

    spec_heat_v = (
        spec_heat_p + gas.P * gas.v / gas.T * dlogV_dlogT_P**2 /
    dlogV_dlogP_T
    )

    gamma = spec_heat_p / spec_heat_v
    gamma_s = -gamma/dlogV_dlogP_T

    return dlogV_dlogT_P, dlogV_dlogP_T, spec_heat_p, gamma_s

```

```

//SIMULATION:
from scipy.integrate import solve_ivp

def vertical_launch(t, y, spec_impulse, mass_prop, time_burn, diameter,
coef_drag):

```

```

'''Evaluates system of time derivatives for velocity, altitude, and
mass.
'''
radius_earth = 6378.388 * 1e3
gravity_ref = 9.80665
density_ref = 1.225
pressure_ref = 101325
gamma = 1.4
height_den = 10400
height_pres = 8400

v = y[0]
h = y[1]
m = y[2]

gravity = gravity_ref * (radius_earth / (radius_earth + h))**2
density = density_ref * np.exp(-h / height_den)
pressure = pressure_ref * np.exp(-h / height_pres)

mach = v / np.sqrt(gamma * pressure / density)
area = np.pi * diameter**2 / 4
drag = 0.5 * density * v**2 * area * coef_drag(mach)

dmdt = -mass_prop / time_burn
dvdt = (-spec_impulse * gravity_ref / m) * dmdt - drag / m - gravity
dhdt = v

return [dvdt, dhdt, dmdt]

# given constants
spec_impulse = 250
mass_initial = 12700
mass_propellant = 8610
time_burn = 60
diameter = 1.626

sol = solve_ivp(
    vertical_launch, [0, time_burn], [0, 0, mass_initial],
method='RK45',
    args=(spec_impulse, mass_propellant, time_burn, diameter,
coefficient_drag),
    dense_output=True
)

```

Adiabatic combustion

CEA also supports calculating the chamber temperature (along with composition) for adiabatic combustion, both with gaseous and liquid propellants.

Cantera's equilibrium solver that we used above handles constant enthalpy and pressure equilibrium ([HP](#)) just fine with gaseous reactants, but how to

CEA has a database of reactants with assigned enthalpies, as described by Gordon and McBride [[GM94](#)]:

- non cryogenic reactants are represented via enthalpy of formation (i.e., heat of formation) at the standard reference temperature of 298.15 K
- cryogenic liquid reactants are represented via enthalpies given at their boiling points, which represent the standard enthalpy of formation minus the sensible heat (between 298.15 K and the boiling point), the heat of vaporization at the boiling point, and also the difference in enthalpy due to real gas effects at the boiling point.

The system analyzes **propellant displacement using a pressurized gas** (e.g., helium or nitrogen).

```
Inputs:  
pp = propellant pressure  
pg = residual gas pressure  
p0 = initial gas pressure  
T0 = gas temperature  
Vp = volume displaced by the propellant  
R = specific gas constant  
ηt = turbine efficiency  
cp = specific heat at constant pressure  
k = heat capacity ratio (k = cp/cv)  
p1, p2 = turbine inlet/outlet pressures  
T1 = turbine inlet temperature  
mt_dot = mass flow rate through turbine  
  
Isothermal Process:  
V0 = (pp / (p0 - pg)) * Vp  
m0 = (pp * Vp) / (R * T0 * (1 - (pg / p0)))  
  
Turbine Power:  
Δh = cp * T1 * [1 - (p2 / p1) ^ ((k - 1) / k)]  
Pt = ηt * mt_dot * Δh  
  
Isentropic Process:  
Solve for V0 from:  
(V0 + 0.180) / V0 = (p0 / pp)^(1/k)
```

Two processes are modeled:

- **Isothermal** (constant temperature).
- **Isentropic** (reversible and adiabatic).

The **ideal gas law** and **mass conservation** are applied.

The algorithm calculates:

- Initial gas volume V_0 ,
- Total gas mass m_0 ,
- Turbine power output P_t .

A. V. FROLOV AND U.-L. PEN

PHYSICAL REVIEW D **68**, 124024 (2003)

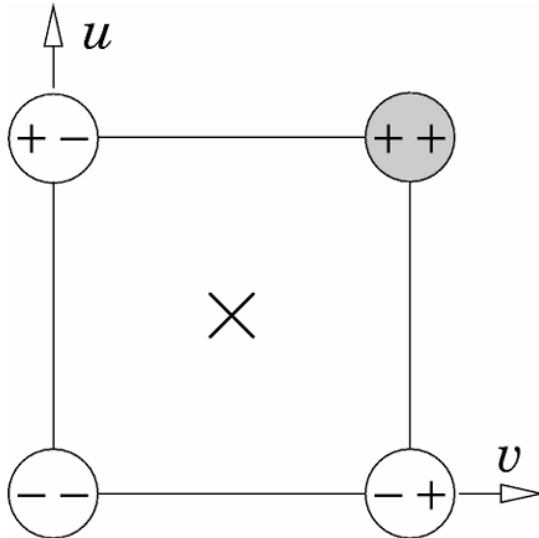
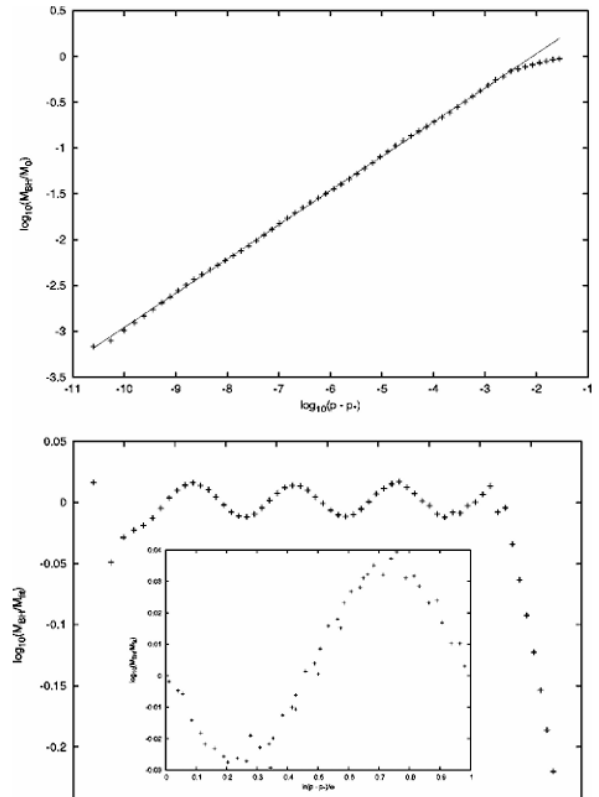


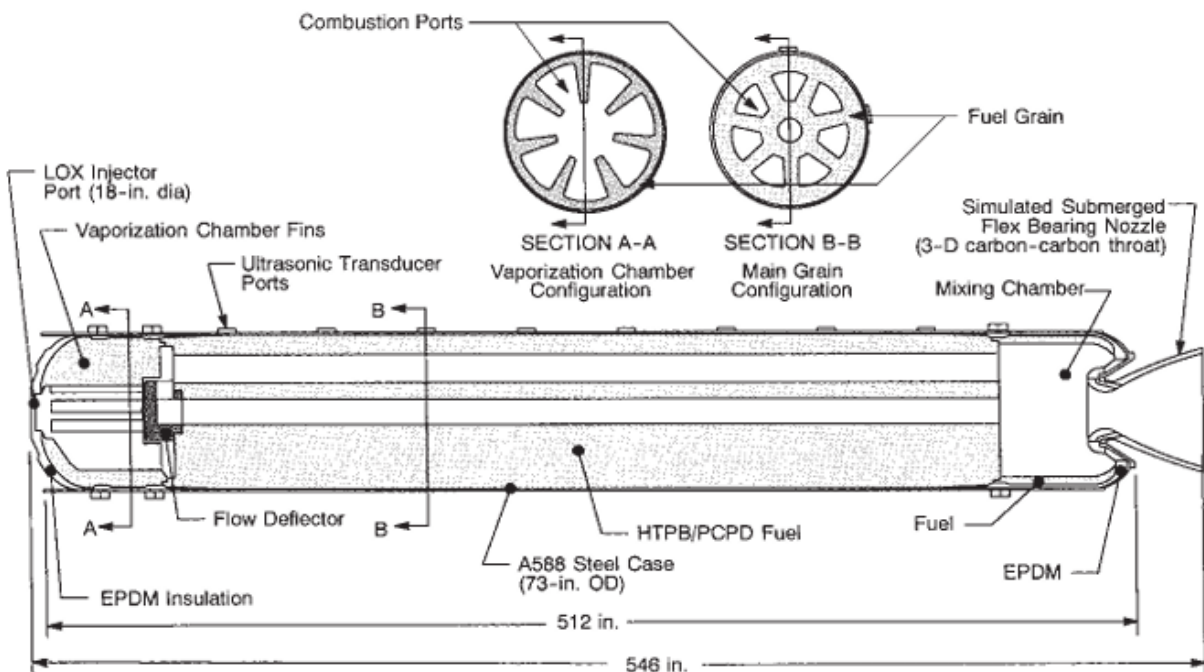
FIG. 3. Discretization on a (u, v) grid.

$$\nabla r \cdot \nabla \phi = 0, \quad \sigma = -\frac{1}{2} \ln (\nabla r)^2 \quad (13)$$

is used to calculate the values of the fields in the center.

V. RESULTS





Maximum operating pressure	900 psia
Maximum vacuum thrust	250,000 lbf
Throat diameter, initial	14.60 in.
Nozzle expansion ratio, initial	12
Liquid oxygen flow rate	420–600 lbm/sec (throttling)
Fuel weight	45,700 lbf
Burn time	80 sec

FIGURE 16–4. Simplified depiction of an experimental 250,000 lbf thrust, hybrid booster with a vaporization chamber, aft mixing chamber and two different solid fuel grains. The vaporization chamber fins and flow deflector are designed to promote flame holding in combustion ports. The fuel ingredient PCPD is polycyclopentadaine.

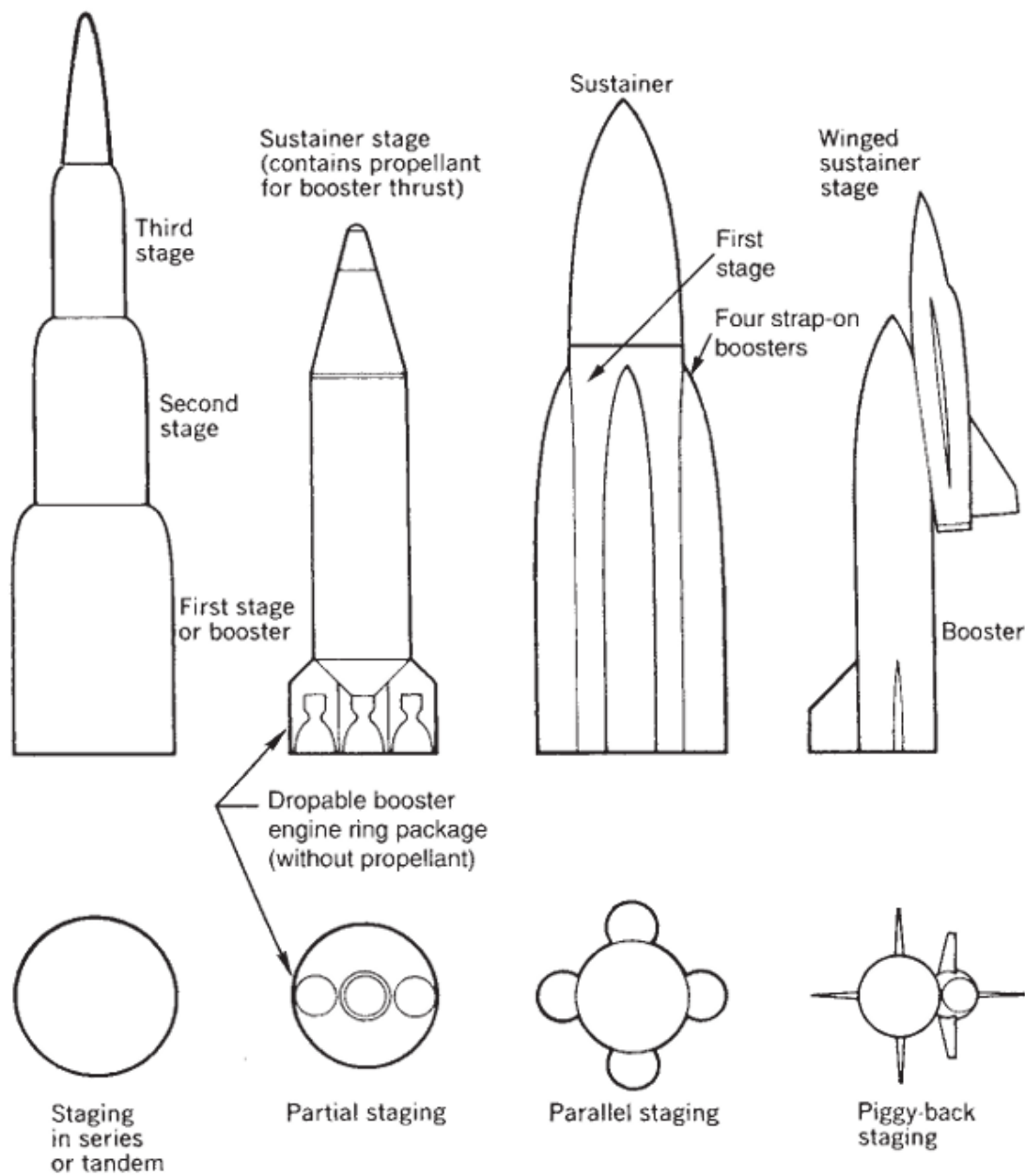
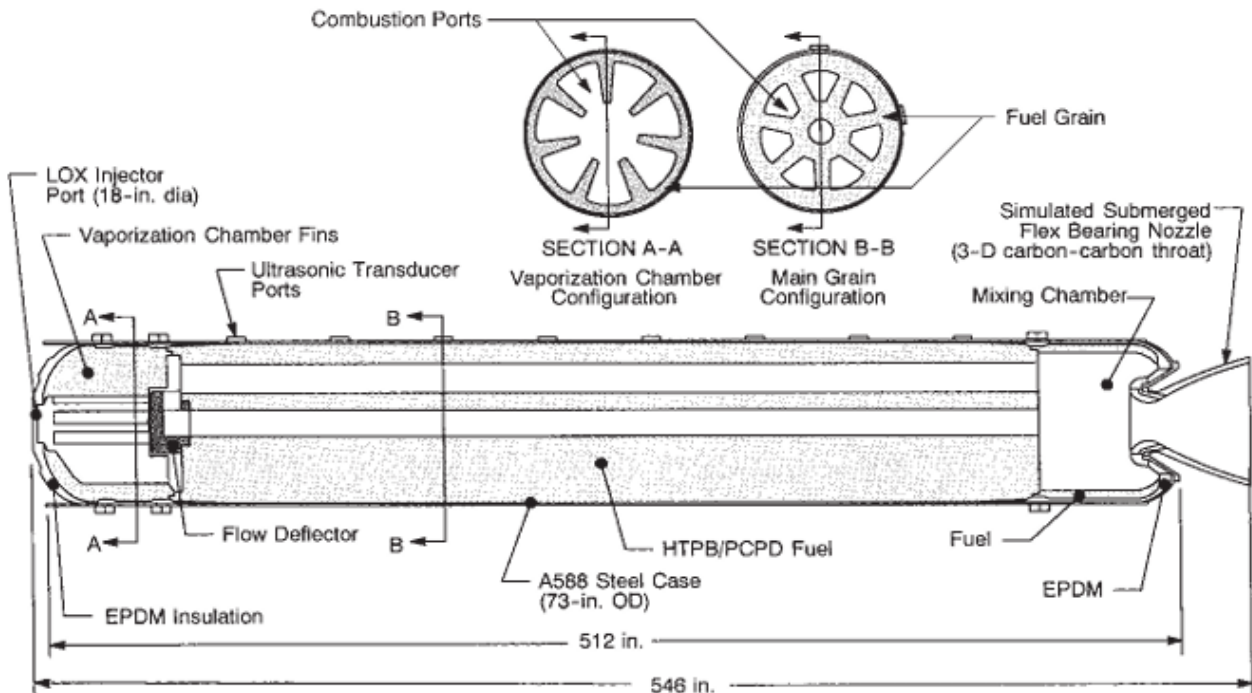


FIGURE 4-15. Schematic renditions of four different geometric configurations for assembling individual stages into a launch vehicle.

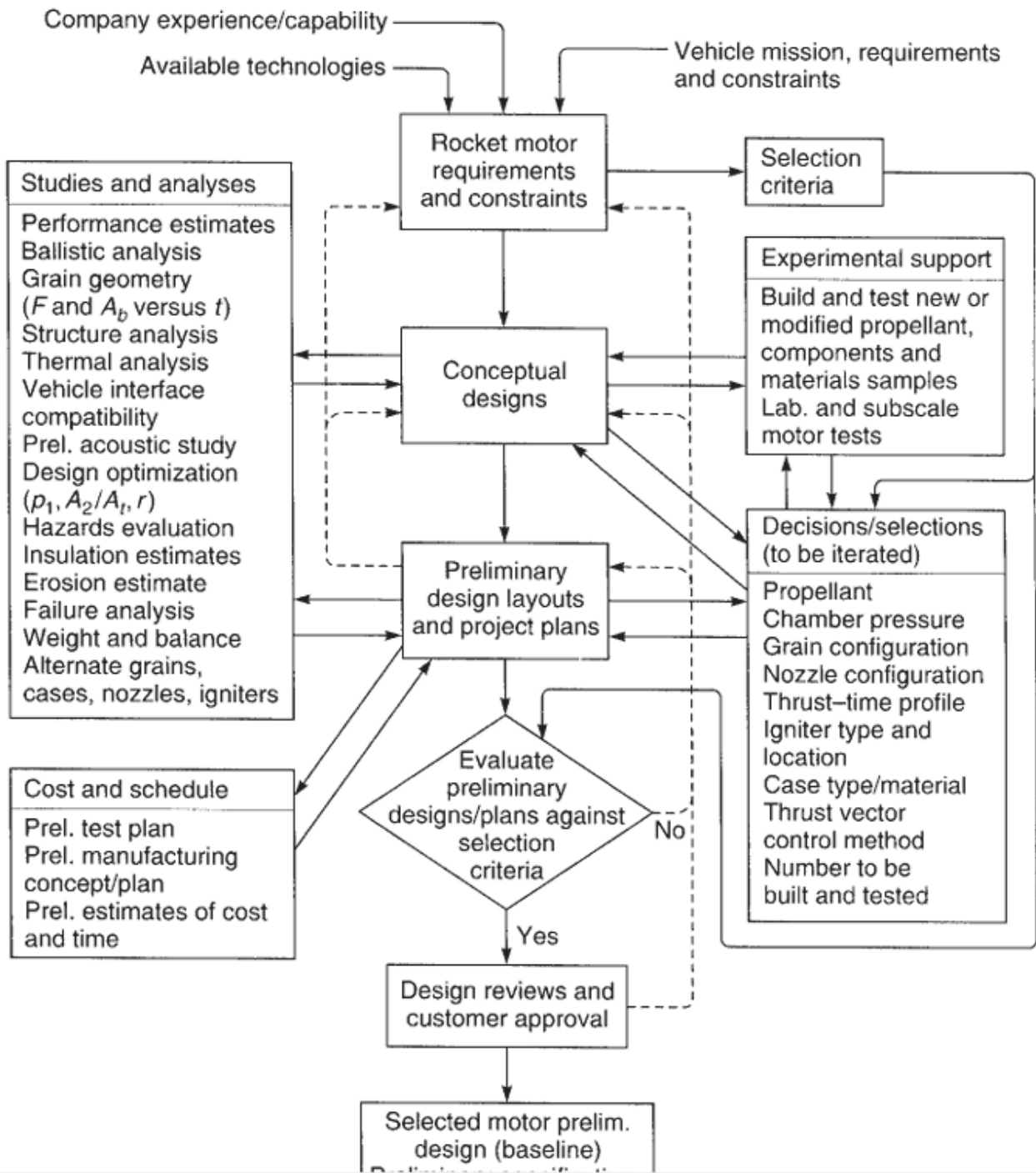


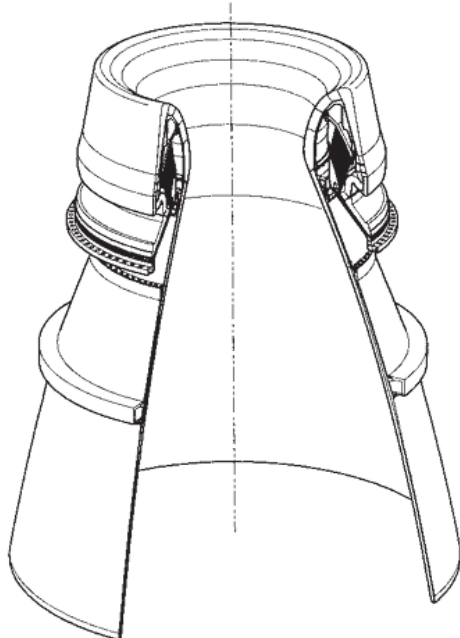
Maximum operating pressure	900 psia
Maximum vacuum thrust	250,000 lbf
Throat diameter, initial	14.60 in.
Nozzle expansion ratio, initial	12
Liquid oxygen flow rate	420–600 lbm/sec (throttling)
Fuel weight	45,700 lbf
Burn time	80 sec

FIGURE 16–4. Simplified depiction of an experimental 250,000 lbf thrust, hybrid booster with a vaporization chamber, aft mixing chamber and two different solid fuel grains. The vaporization chamber fins and flow deflector are designed to promote flame holding in combustion ports. The fuel ingredient PCPD is polycyclopentadaine.



FIGURE 16–3. SpaceShipOne gliding down for landing. This air ship uses a hybrid propulsion system to produce its main thrust. The propellant is N₂O-HTPB. (Photo by scaled composites. SpaceShipOne is a Paul G. Allen Project © Mojave Aerospace Ventures, LLC.)





RSRM Nozzle Characteristics

Type	Contoured or bell
Thrust vector control	Flexible bearing
Expansion area ratio	7.72
Throat diameter	53.86 in.
Exit diameter	149.64 in.
Total length	178.75 in.
Nozzle weight	23, 941 lbf
Maximum pressure	1.016 psi
Maximum thrust (vac.)	3, 070, 000 lbf
Burn time	123.7 sec
Materials	
Housings	Steel and aluminum
Liners	Carbon cloth phenolic

FIGURE 15–8. External quarter section view of nozzle configuration of the historic Space Shuttle reusable solid rocket motor (RSRM). Courtesy of Orbital ATK

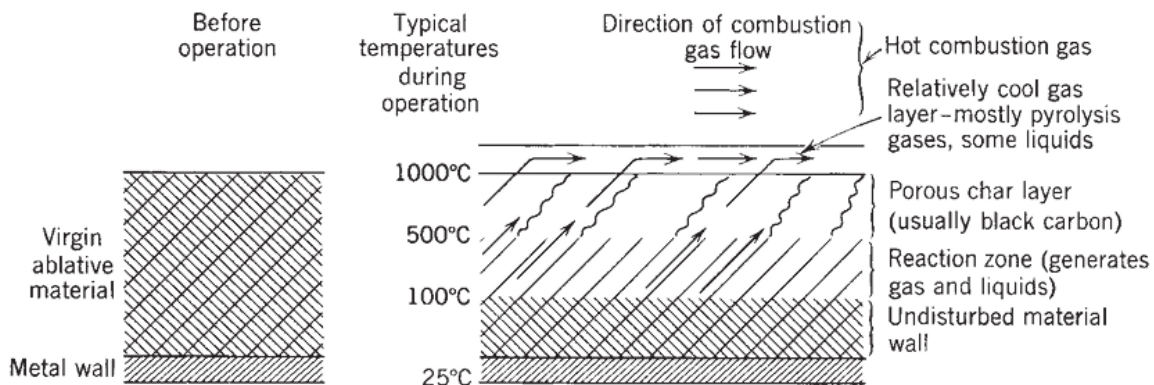


FIGURE 15–11. Zones in an ablative material during rocket operation with two sets of fibers (seen as multiple lines) at 45° to the flow.

Theoretical specific impulse (vacuum conditions)	278.1 sec
Delivered average specific impulse (vacuum conditions)	268.2 sec
<i>Losses (calculated):</i>	(9.9 sec total)
Two-dimensional two-phase flow (includes divergence angle loss)	7.4 sec
Throat erosion (reduces nozzle area ratio)	0.9 sec
Boundary layer (wall friction)	0.7 sec
Submergence (flow turning)	0.7 sec
Finite rate chemistry (chemical equilibrium)	0.2 sec
Impingement (of Al_2O_3 particles on nozzle wall)	0.0 sec
Shock (if turnback angle is too high or nozzle length too low)	0.0 sec
Combustion efficiency (incomplete burning)	0.0 sec

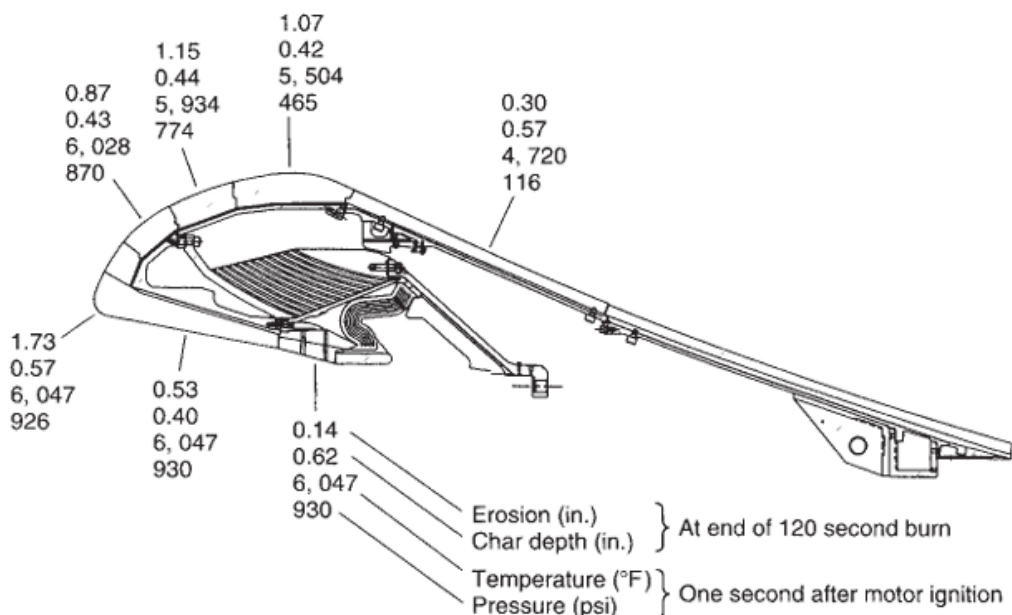


FIGURE 15–10. Erosion measurements and char depth data of the carbon fiber phenolic material of the nozzle of the Space Shuttle Reusable Solid Rocket Motor. Courtesy of Orbital ATK

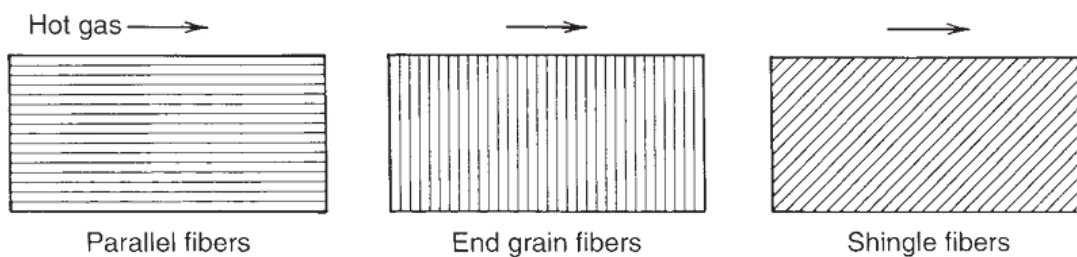


FIGURE 15–12. Simplified sketches of three different types of fiber-reinforced ablative materials.

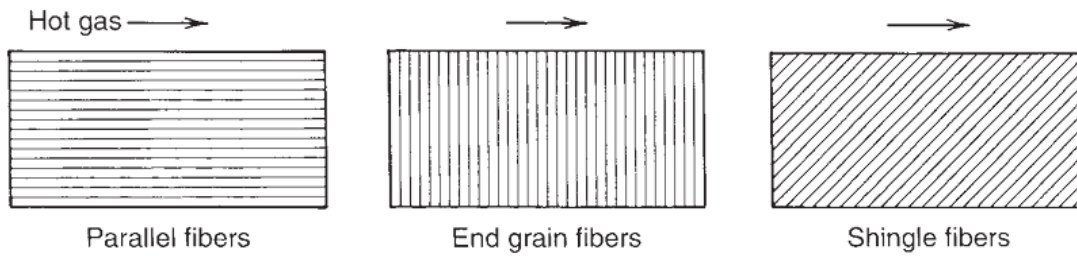


FIGURE 15–12. Simplified sketches of three different types of fiber-reinforced ablative materials.

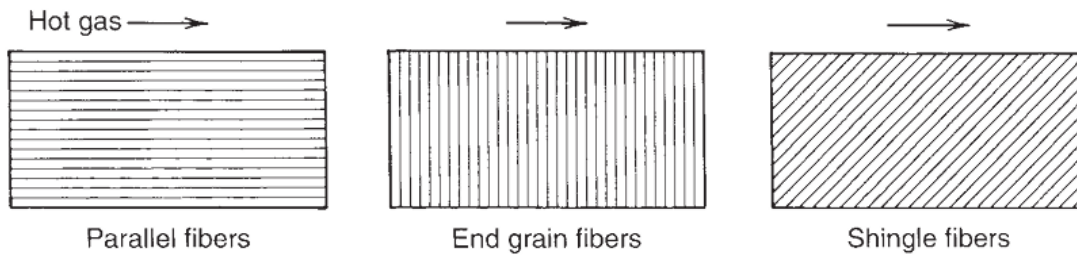


FIGURE 15–12. Simplified sketches of three different types of fiber-reinforced ablative materials.

SOLID ROCKET MOTOR COMPONENTS AND DESIGN

